observe modulation of the dipolar coupling by MAS.

Acknowledgment. We express our appreciation to the Monsanto Co. for permission to publish this work and to Jacob Schaefer for his guidance and advice.

References and Notes

(1) Hill, R. *J. Mech. Phys. Solids* **1956**, *13*, 189.
(2) Bander, B. W. *J. Appl. Polym. Sci.* **1965**, *9*, 2887.
(3) Flory, P. J. *Principles of Polymer Chemistry*; Cornell University: Ithaca, NY, 1978; p 580.
(4) Morbitzer, L.; Kranz, D.; Humme, G.; Ott, K. H. *J. Appl. Polym. Sci.* **1976**, *20*, 269.
(5) Kambour, R. P. *J. Polym. Sci., Macromol. Rev.* **1973**, *7*, 1.
(6) Jelinski, L. W.; Dumas, J. J.; Watnick, P. I.; Bass, S. V.; Shepherd, L *J. Polym. Sci.* **1982**, *20*, 3285.
(7) Dutch, M. W.; Grant, D. M. *Macromolecules* **1970**, *3*, 165.
(8) Schaefer, J. *Macromolecules* **1971**, *5*, 427.
(9) Schaefer, J.; Chin, S. H.; Weissman, S. I. *Macromolecules* **1972**, *6*, 798.
(10) English, A. O.; Dybowski, C. *Macromolecules* **1984**, *17*, 446.
(11) Brown, D. R.; Munie, G. C.; Jonas, J. *J. Polym. Sci., Polym. Phys. Ed.* **1982**, *20*, 1659.
(12) Bergmann, K.; Geberding, K. *Colloid Polym. Sci.* **1981**, *259*, 990.
(13) Rowland, T. J.; Labun, L. C. *Macromolecules* **1978**, *11*, 466.
(14) Cohen-Addad, J. P.; Faurie, J. P. *J. Chem. Phys.* **1974**, *61*, 1571.
(15) Stejskal, E. O.; Schaefer, J.; Waugh, J. S. *J. Magn. Reson.* **1977** *28*, 105.
(16) Meiboom, S.; Gill, D. *Rev. Sci. Instrum.* **1958**, *29*, 6881.
(17) Firestone Tire and Rubber Co. Product Bulletin, August 1973.
(18) Seely, S. *Radio Electronics*; McGraw-Hill: New York, 1956; pp 380–384.
(19) Olver, F. W. J. *Handbook of Mathematical Functions*; Abramowitz, M., Stegun, I. A., Eds.; Applied Mathematics Series 55; National Bureau of Standards: Washington, DC, 1964; p 385.

Scattering Function of Polystyrene

M. Rawiso*

Institut Laue Langevin, 38042 Grenoble Cedex, France

R. Duplessix and C. Picot

Institut Charles Sadron (CRM-EAHP), 67083 Strasbourg Cedex, France.
Received April 24, 1986

ABSTRACT: An improvement over previous determinations of the structure factors of polystyrene has been obtained from small-angle neutron scattering by using the isotopic labeling method. Atactic polystyrenes have been deuteriated in three different ways: in the backbone, in the phenyl rings, or in both. Their scattering functions, measured from dilute solutions in a good solvent, are found to be quite different beyond $q = 0.05$ Å^{-1}. Actually, the variations with contrast of the structure factor indicate that the monomer structure affects the scattering function of polystyrene beyond q values as low as 0.03 Å^{-1}. To interpret this result, the polystyrene is approximated by a curved cylinder, and the effect of its local structure is divided into two parts. First, the properties of the monomer species are smoothed along an infinitely thin curve. This object is represented by the Porod–Kratky chain model. Second, the effect of side groups on the scattering function is treated as a simple thickness; a corrective term $\Phi(q)$ is then added to the structure factor $S_0(q)$ of the thin thread. The cross-section term $\Phi(q)$ is determined for each type of deuteriated polystyrene. Remarkably, these functions are not compatible with a model where the chain has cylindrical symmetry; therefore, anisotropic correlations between the orientations of successive phenyl groups must be important. The structure factor of the thin thread follows the $q^{-1/\nu}$ decay of the self-avoiding random walk model up to $q = 0.06$ Å^{-1}; beyond this point the rigidity of the chain becomes important. A universal constant related to the amplitude of this $q^{-1/\nu}$ decay is determined.

I. Introduction

The only direct methods available for studying the conformational statistics of chain molecules are radiation scattering techniques.[1,2] They yield the structure factor $S(\vec{q})$, defined as the Fourier transform of the monomer density autocorrelation function $\langle\rho(\vec{r})\rho(0)\rangle - \langle\rho\rangle^2$.[3] In the static approximation, the magnitude of the scattering vector $\vec{q}$ is related to the wavelength of the radiation λ and the angle between incident and scattered beams θ by the relation

$$q = \frac{4\pi}{\lambda} \sin \frac{\theta}{2} \tag{1}$$

For chain molecules that can take random orientations, we are concerned with the isotropic average $S(q)$ defined as

$$S(q) = \frac{1}{4\pi} \int_0^{4\pi} S(\vec{q})\, d\Omega$$

and the aim is to obtain this function for a single molecule at all q values. A reciprocal Fourier transform will then yield the pair correlation function of monomers $\langle\rho(\vec{r})\rho(0)\rangle$ which describes the average conformation of the chain.

From an experimental point of view, this procedure is unrealistic because the range of q values is always limited; its upper boundary sets the spatial resolution of the experiment.[3,4] Two distinct approaches are then used.

(1) The Guinier range, i.e., small q values: for homopolymers, we measure the mean square radius of gyration of the chain R_G^2. Some details about the chain statistics can be obtained by studying R_G^2 as a function of the molecular weight M_w. This requires well-characterized samples in a broad range of M_w values.

(2) The range of higher q values, i.e., for $qR_G > 1$: the spatial resolution is improved, and we observe the corre-

* Address correspondence to this author at the Laboratoire de Physique des Solides, Université Paris Sud, 91405 Orsay, France.

0024-9297/87/2220-0630$01.50/0

lations inside the chain on a scale that stretches down to the monomer size. This method has a distinct advantage in that statistical laws can be obtained from one sample, and these reflect directly the pair distribution of monomers. The strategy is then to compare experimental curves with predicted scattering functions according to the different models that seem to be realistic.

In the past few years, following these two methods, a rather complete set of experimental scattering functions has been obtained for flexible polymers, using the light and X-ray scattering techniques for dilute solutions and the neutron scattering technique for higher concentrations and melts.

We are concerned here with the second approach, where most of the experiments have been analyzed by use of random walk and self-avoiding random walk models which lead to universal scattering behaviors in the sense that they do not take into account the local structure of the chain. In this analysis the spatial scales of the experiments were assumed to correspond to the so-called intermediate range of scattering vectors. Unfortunately, with neutron and X-ray scattering techniques this is not necessarily correct.

This last point can be illustrated with polystyrene. In dilute solutions, the structure factor of the chain has been found to be proportional to q^{-2} and $q^{-1/\nu}$ for poor and good solvents, respectively,[5-10] ν being the excluded volume exponent.[11-13] In isotropic melts, a q^{-2} scattering behavior has been observed.[14,15] A remarkable fact is that these laws, characteristic of the random walk and self-avoiding random walk models, have been found to be valid even for q values beyond 0.1 Å^{-1}. This is quite surprising since on this scale the local structure of the polystyrene should be observable, and therefore universal laws should no longer apply. Indeed direct calculations of the structure factor[16] lead to different results: the scattering functions of flexible polymers are found to be extremely sensitive to local configurations beyond $q = 0.03$ Å^{-1}. This has been checked through X-ray[17] and neutron[18] scattering experiments on poly(methyl methacrylate). Yet for polystyrene many authors still consider q values up to 0.1 Å^{-1} to belong to the intermediate range of scattering vectors. Thus crossover effects between universal behaviors have been suggested to explain the scattering curves in a q range close to the inverse of the statistical length.[19]

Most of the confusion stems from the following question: should polystyrene be approximated by an infinitely thin thread? As shown in Figure 1, this assumption depends on the spatial resolution achieved with the scattering experiment. On a local scale, it is expected to be wrong because the monomer is no longer a point scatterer. Accordingly, to understand why the local structure of the polystyrene appears to have no influence on its structure factor, the effect of the cross section of the chain should be studied first. For this, the chemical resolution can be improved by using isotopic labeling on different parts of the monomer unit. More precisely, to determine the structure factor of polystyrene, we have used three different kinds of deuteriated atactic polystyrenes having the following chemical formulas: fully deuteriated, $PSD_8 \rightarrow -(CD_2CDC_6D_5)_n-$; deuteriated in the phenyl rings, $PSD_5H_3 \rightarrow -(CH_2CHC_6D_5)_n-$; deuteriated in the backbone, $PSD_3H_5 \rightarrow -(CD_2CDC_6H_5)_n-$ and $PSD_2H_6 \rightarrow -(CDHCDC_6H_5)_n-$.

The conformational statistics are the same for these four polymers, but, for neutron scattering, the contrast factors of various parts of the monomers are different. Thus it will be possible to know whether local structure effects are actually present or not in the q range over which universal scattering behaviors have been previously claimed.

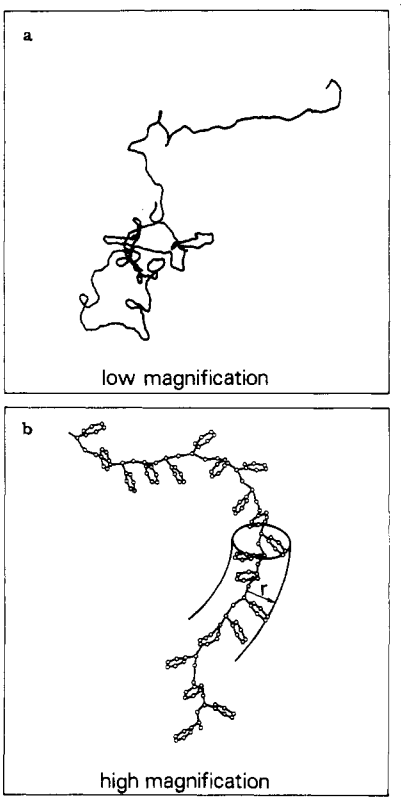

Figure 1. 2d representations of the structure of polystyrene; two spatial resolutions are considered. (a) Spatial scale much larger than the size of the phenyl rings; the chain can be represented by a smooth curve in space. (b) Local scale: the cross section of the chain is no longer negligible, and the structure of the chain can be approximated by a curved cylinder of radius $r = 4$ Å.

Our measurements have been performed on dilute solutions in carbon disulfide, which is a good solvent for these polystyrenes.

II. Experimental Evidence for the Effect of the Local Structure on the Scattering Function of Polystyrene

In this section we present typical results. Section III contains all experimental details.

We report the scattering functions for the three kinds of deuteriated polystyrenes measured on an absolute scale in the q range $0.01 < q < 0.6$ Å^{-1}. Because we observe pair correlations between monomers within the chain, we are mainly interested in the dimensionless scattering function $g(q)$ defined as

$$g(q) = (m/cN)S(q) \tag{2}$$

where $S(q)$ is the chain structure factor per unit volume (cm^{-3}), m the molar mass of monomers (g mol^{-1}), c the concentration of the polymer (g cm^{-3}) and N Avogadro's number (mol^{-1}).

$P(q)$ being the structure factor defined by $P(q) = S(q)/S(0)$, which is widely used for light scattering experiments, we have the relationship

$$g(q) = (M_w/m)P(q) \tag{3}$$

where M_w is the molecular weight of the macromolecule (g mol^{-1}). At high q values, $g(q)$ has the advantage of being universal with respect to the chain contour length and the molar mass of monomers. If we assume that the isotopic exchange H–D does not disturb the thermodynamics of the system and the electronic state of the monomers, the same interactions are involved for the three kinds of deuteriated polystyrenes. Therefore their structure factors

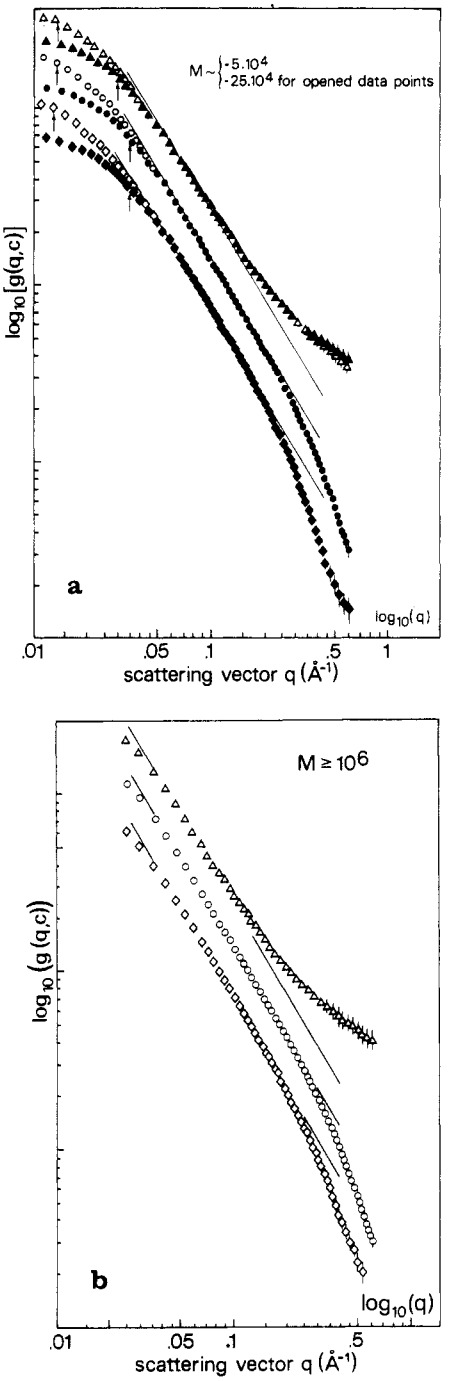

Figure 2. Double-logarithmic plot of the scattering curves $g(q,c)$ for selectively deuteriated polystyrenes in dilute solution of CS_2: (○) fully deuteriated; (◇) deuteriated in the phenyl rings; (△) deuteriated in the backbone. The scattering curves are shifted in an arbitrary way along the y axis to allow a convenient comparison between them. The straight lines have a slope $\alpha = 1/\nu$ ($\nu = 0.588$). Arrows indicate the q values corresponding to $qR_G = 3$. (a) Molecular weights close to 5×10^4 and 2.5×10^5: PSD_8-1 and -2, PSD_5H_3-2 and -3, and PSD_3H_5-2 and -3. $c = 0.025$ g cm^{-3}. (b) Molecular weights $M_w \geq 10^6$: PSD_8-3, PSD_5H_3-4, and PSD_2H_6-1. $c = 0.02$ g cm^{-3}.

should be identical if the thin thread model can be used to represent the macromolecule.

For a finite concentration c, the measured scattering function is rather $g(q,c)$, which does not correspond to the structure factor of one single molecule. For a dilute solution we can write in the intermediate and asymptotic ranges of scattering vectors:

$$g(q,c) = g(q) + g_2(q,c) \quad (4)$$

Here $g(q)$ is the intramolecular term that depends on the molecular weight and on the type of labeling, while $g_2(q,c)$ is the intermolecular term that depends on the concentration and the molecular weight but not on the labeling (see section III.B.4). Consequently, the previous statement given for $g(q)$ remains valid for $g(q,c)$ if polymer solutions of identical concentration and molecular weight are compared for different types of labeling.

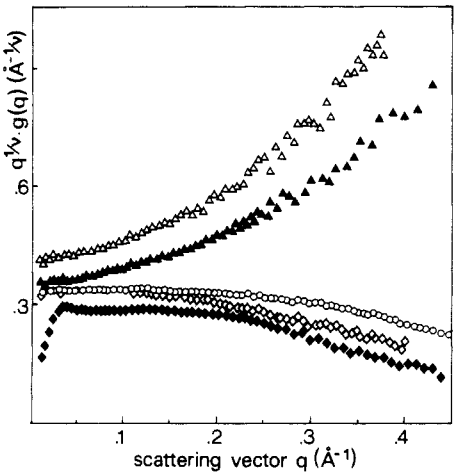

Figure 3. Intramolecular terms $g(q)$ for selectively deuteriated polystyrenes in dilute solution of CS_2. Data are given on an absolute scale in a modified Kratky plot that takes into account the excluded volume effect ($\nu = 0.588$): (○) fully deuteriated (PSD_8-3); (◇) deuteriated in the phenyl rings (PSD_5H_3-4 and PSD_5H_3-2 for opened and filled data points, respectively); (△) deuteriated in the backbone (PSD_2H_6-1 and PSD_3H_5-3 for opened and filled data points, respectively).

The scattering functions $g(q,c)$ for the three kinds of deuteriated polystyrenes are presented in Figure 2. For each molecular weight they are quite different, and, as indicated above, this arises from the intramolecular term. We conclude that the polystyrene is similar to an inhomogeneous particle on the spatial scale of the experiment.

For fully deuteriated polystyrenes the $q^{-1/\nu}$ scattering behavior observed previously[7,9,10] is found again up to $q = 0.2$Å^{-1}, with $\nu = 0.588$.[20] The same power law is observed for polystyrenes deuteriated in the phenyl rings up to $q = 0.15$ Å^{-1}. However, contrary to previous assertions, these scattering behaviors are not explained by the self-avoiding random walk model. Indeed, polystyrenes deuteriated in the backbone, which are the closest approximations to the object described by the model (see section III.B.1), have different structure factors. Those are proportional to $q^{-\beta}$ with $\beta < 1/\nu$, which is not due to the excluded volume interaction but rather to the effect of the local structure of the chain.[21] We shall argue that the $q^{-1/\nu}$ scattering behavior observed with fully deuteriated polystyrenes for q values as high as 0.1 Å^{-1} can be explained by the balance of two local effects: the rigidity of polystyrene and the side extension of its phenyl rings.[22]

Still one could argue that the $q^{-1/\nu}$ scattering behavior should still be observed at smaller q values because the local structure of the chain is no longer resolved. However, for finite concentration this effect is obscured by intermolecular correlations, as shown in Figure 2a. Thus we have separated out these intermolecular correlations (section III.B.4), and the resulting intramolecular terms $g(q)$ are presented in Figure 3. They do indeed show the characteristic $q^{-1/\nu}$ scattering behavior at small q values. The fact that the absolute heights of the $q^{-1/\nu}$ plateaus appearing in Figure 3 are not identical will be explained later (see section III.B.2,4). However, it is clear that the q range where the local properties of the chain can be neglected is much smaller than previously thought. It

Table I
Characteristics of Polystyrene Samples

sample	M_w	M_w/M_n	τ, % D	$\bar{v}$ at 20 °C, cm^3 g^{-1}	c^*, g cm^{-3}
PSD_8-1	53 500	1.15	>99		0.151
PSD_8-2	257 500	1.12	>99	0.857	0.043
PSD_8-3	1 280 400	1.15	>99		0.012
PSD_5H_3-1	49 900	1.25	τ_ϕ ~95		0.152
PSD_5H_3-2	47 800	1.3	~97	0.875	0.157
PSD_5H_3-3	261 700	1.3	~97	0.874	0.040
PSD_5H_3-4	955 800	1.21	~99	0.878	0.014
PSD_3H_5-1	63 000	1.3	τ_ϕ <5		0.123
PSD_3H_5-2	62 500	1.4	<5	0.894	0.124
PSD_3H_5-3	239 200	1.16	<5	0.893	0.042
PSD_2H_6-1	1 628 600	1.23	τ_B ~70	0.902	0.009
PSH_8				0.922	
CS_2				0.792	

extends at most up to 0.05 Å^{-1} and not to values as high as 0.2 Å^{-1}, as would have been suggested by considering the results for fully deuteriated polystyrenes alone.

These results challenge some crossover studies performed on the structure factors of polystyrene, like the display of the thermal blob.[19] More generally, the main theoretical models for chain molecules are concerned with one-dimensional curves in space. Therefore, in order to check the theories and measure some parameters like radius of gyration or statistical length, it is necessary to show that the side extension of the chains can be neglected.

The next sections are devoted to the detailed measurements of the scattering functions and to the analysis of the effects of local rigidity and side extension of the chain. Finally, we wish to determine the structure factor of the thin thread associated with polystyrene.

III. Detailed Measurements of the Scattering Functions

A. Experimental Procedures. 1. Samples. Neutron scattering experiments were made on atactic polystyrenes deuteriated in four different ways, PSD_8, PSD_5H_3, PSD_3H_5, and PSD_2H_6, with three classes of molecular weights, $M_w \sim 5 \times 10^4$, $M_w \sim 2.5 \times 10^5$, and $M_w \geq 10^6$.

Fully deuteriated polystyrenes PSD_8 were prepared by anionic polymerization under high vacuum[23] of styrene D_8. Polystyrenes deuteriated either in the backbone or in the phenyl rings were prepared by two distinct methods depending on the molecular weight.

For low molecular weights (5×10^4 and 2.5×10^5), the isotopic exchange was carried out on the polymer. Polystyrenes deuteriated in the backbone PSD_3H_5 were obtained from perdeuteriated polystyrenes PSD_8 by catalytic deuterium exchange of the phenyl groups in benzene solution;[24] the catalyst was ethylaluminum dichloride, $Cl_2AlC_2H_5$. The same procedure yielded polystyrenes deuteriated in the phenyl rings PSD_5H_3 from solutions of hydrogenated polystyrenes PSD_8 in deuteriated benzene.

For high molecular weights ($\geq 10^6$), the above methods cannot be used because they lead to chain scission; therefore, selectively deuteriated styrene molecules were first prepared and then polymerized.[25] Following this procedure the polystyrene deuteriated in the backbone has, on average, only two deuterium atoms located in the α and β positions in the chain skeleton. It is described by the chemical formula PSD_2H_6 or $-(CDHCDC_6H_5)_n-$, although the D/H ratio for the β position is close to 1.1, as shown by deuterium NMR.

2. Characterization of Samples. The degree of deuteriation of each kind of polystyrene was determined by using proton NMR with a 90-MHz Perkin-Elmer spectrometer. For polystyrenes deuteriated in the backbone this method is not accurate, but we have obtained consistent results with the densimetry method. Moreover, for the high molecular weight samples PSD_5H_3 and PSD_2H_6, deuterium NMR was also used. The exchange ratio was found to be of the order of 97% for PSD_5H_3 samples with low molecular weights, whereas only a lower limit of 95% can be given for PSD_3H_5 samples. In order to compute the contrast factors involved in neutron scattering experiments, we have measured the specific volumes of each kind of polystyrene at 20 °C for 2% by weight in carbon disulfide. The experiments were performed with a Paar DMA 601 M digital densimeter with an accuracy of better than 0.5%. In the case of partially deuteriated monomers, lower values are observed with respect to those obtained from a simple additivity law. For PSD_3H_5 samples, according to the isotopic exchange reaction, such a difference can be related to an exchange ratio less than 1; for PSD_5H_3 samples this is not possible. However, this does not affect the neutron contrast factors calculated through the additivity law (within 1%). On the other hand, the neutron contrast factors depend on the degree of deuteriation of the macromolecules.

The polydispersity of samples was characterized by gel permeation chromatography and the different average molecular weights: M_n, M_w, and M_z, have been derived from the so-called "universal" calibration.[26] The molecular weight accuracy is 7%.

The overlap concentrations, which define regions of crossover between dilute and semidilute regimes, were obtained from the relation

$$c^* = M_w/NR_G^3$$

where N is Avogadro's number. For perdeuteriated polystyrenes, the radii of gyration were deduced from the law R_G (Å) = 0.122 $M_w^{0.6}$, as determined by using a least-squares fit of previous experimental data.[15] For the other kinds of labeling this law was corrected to take into account the molar masses, which are different.

Table I lists the main characteristics of the samples used in this study.

3. Scattering Geometries and Measurements. The neutron scattering experiments were performed at ILL in Grenoble, France. The spectrometers D 17, D 1B, and D 16 were used. The range of scattering vectors covered, the spread in the wavelength of the incident neutrons $\Delta\lambda/\lambda$, and the resolution Δq due to the divergence of the incident beam are given in Table II for each instrument. With regard to the q range of the D 1B spectrometer, beyond

Table II
Characteristics of the Scattering Geometries

spectrometer	q range, Å^{-1}	$\Delta\lambda/\lambda$, %	Δq, 10^{-3} Å^{-1}
D 17	$0.01 < q < 0.35$	10	3
D 1B	$0.1 < q < 1.5$	1	7.5
D 16	$0.06 < q < 0.6$	<2	14.

$q = 0.6$ Å^{-1} it is no longer possible to neglect density fluctuations and therefore to use the contrast factor concept;[27] also the signal-to-noise ratio of our experiments was then too low. Data obtained at high q values were used only to check that background subtractions were achieved in a correct way.

Our measurements were carried out at room temperature on dilute solutions of the polystyrene in carbon disulfide. The main advantage of this solvent is that it gives no incoherent scattering and therefore the signal-to-noise ratio is good even in the case of low contrast. This improves the accuracy at high q values.

For samples with low molecular weights (5×10^4 and 2.5×10^5) the polymer concentration was $c = 0.025$ g cm^{-3}. For samples with high molecular weights ($\geq 10^6$) two concentrations have been used: $c = 0.02$ and 0.004 g cm^{-3}. With the lower concentration, intermolecular correlations were negligible in the whole experimental q range.

Sample holders were quartz cells of 5-mm thickness except for H_2O, whose thickness was 1 mm. Multiple scattering effects were quite negligible, as shown by the comparison with the data obtained by using quartz cells of 2-mm thickness.

B. Data Analysis. All data were treated according to standard ILL procedures for small-angle isotropic scattering. After radial averaging, the spectra were corrected for absorption and sample thickness. The scattering from the empty cell was subtracted, and normalization to the unit incident flux, geometrical factors, and detector cell efficiency corrections was performed by using the scattering of H_2O or vanadium (for D 1B). The data were put on an absolute scale by introducing the differential cross section per unit volume of H_2O, $\Sigma_{\text{Imm}}^{H_2O}$ (cm^{-1}). This term is known at room temperature for different wavelengths from the instrumental calibrations that have been performed by using various standard samples.[28] With this procedure absolute measurements are achieved with an accuracy better than 8%. In this way, the differential cross section per unit volume $\Sigma(q)$ (cm^{-1}) was obtained for each sample. We have

$$\Sigma(q) = \Sigma^{\text{coh}}(q) + \Sigma^{\text{B}} \tag{5}$$

where $\Sigma^{\text{coh}}(q)$ is the coherent differential cross section that contains all the information needed to describe the structure of the sample. Neglecting multiple scattering and density fluctuations, we have

$$\Sigma^{\text{coh}}(q) = K^2 S(q) \tag{6}$$

where K^2 (cm^2) is the contrast factor between the macromolecules and the solvent and $S(q)$ (cm^{-3}) is the scattering function of the chains. The function $g(q)$ used to report our data is then derived from $S(q)$ according to eq 2. Σ^{B} is a flat background due to the scattering of the solvent and the incoherent scattering of the polymer. In order to obtain $\Sigma^{\text{coh}}(q)$, which is the quantity of interest, we have to measure Σ^{B}.

1. Contrasts for Coherent Scattering. As concerns our experiments, neutrons interact with the nuclei in the sample. For small-angle scattering, where the spatial resolution $2\pi/q_{\text{max}}$ is much smaller than molecular dimensions, the elementary scatterers are not atoms but rather molecules or monomer units of macromolecules.

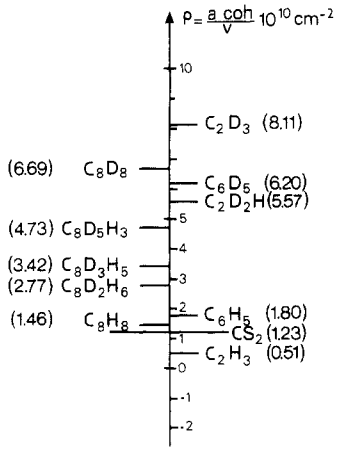

Figure 4. Neutron scattering length densities for polystyrenes deuteriated in different ways in dilute solution of CS_2. On the left, the monomer is taken as elementary scatterer. On the right, the backbone and phenyl parts of the monomer are considered as elementary scatterers: $v = 24.75$ cm^3 mol^{-1} for the backbone and $v = 71.13$ cm^3 mol^{-1} for the phenyl ring.

Indeed, q_{max} being the largest q value probed with the experiment, $2\pi/q_{\text{max}}$ represents the shortest distance that can be resolved. Hence the elementary scatterers of volume v are characterized by the scattering length densities defined as[4,27]

$$\rho = \sum_{\alpha} a_{\alpha}^{\text{coh}}/v. \tag{7}$$

where the summation is over all atoms in volume v and a_{α}^{coh} is the coherent scattering length associated to the α atom.[29]

Figure 4 shows the ρ values relevant for the different kinds of deuteriated polystyrenes used in this study as well as that of the solvent molecule. First we have taken the monomer as elementary scatterer and the value of ρ depends on the labeling. This is acceptable only at low q values, when distances comparable to the dimension of the monomer are not resolved. For higher resolutions we divide the monomer unit into two parts: the backbone $-(CH_2CH)-$ and the phenyl group $-(C_6H_5)$ were taken as elementary scatterers. Here the main problem is to know the volume v occupied by each part of the monomer. These volumes were evaluated by using the law of additivity of partial molar volumes and data given for glassy amorphous polystyrene[30] modified to take into account our densimetry results.

The observed coherent differential cross sections $\Sigma^{\text{coh}}(q)$ is given by eq 6 and is proportional to K^2 with

$$K = v(\rho - \rho_s) \tag{8}$$

where ρ is the scattering length density of the monomers of volume v and ρ_s is that of the solvent. When the solute is treated like a two-component particle, three correlation functions have to be considered: S_{B} for the backbone, S_ϕ for the phenyl rings, and the cross term $S_{\text{B}\phi}$. Relation 6 is then replaced by

$$\Sigma^{\text{coh}}(q) = K_{\text{B}}^2 S_{\text{B}}(q) + K_\phi^2 S_\phi(q) + 2K_{\text{B}}K_\phi S_{\text{B}\phi}(q) \tag{9}$$

with

$$K_{\text{B}} = v_{\text{B}}(\rho_{\text{B}} - \rho_{\text{S}}) \qquad K_\phi = v_\phi(\rho_\phi - \rho_{\text{S}}) \tag{10}$$

where ρ_{B} and ρ_ϕ are the scattering length densities of the backbone and phenyl parts of the monomer of volumes v_{B} and v_ϕ, respectively. K, K_{B}, and K_ϕ defined by eq 8 and 10 are related by the equation

$$K^2 = K_{\text{B}}^2 + K_\phi^2 + 2K_{\text{B}}K_\phi \tag{11}$$

Table III
Neutron Contrast Factors

contrast factor, barn ($=10^{-24}$ cm^2)	PSD_8/CS_2	PSD_5H_3/CS_2	PSD_3H_5/CS_2	PSD_2H_6/CS_2	PSH_8/CS_2
K^2	75.65	31.08	12.24	6.02	0.13
K_B^2	7.99	0.088	7.99	3.18	
K_ϕ^2	34.46	34.46	0.45	0.45	
$2K_BK_\phi$	33.20	-3.47	3.80	2.39	

Table IV
Effective Neutron Contrast Factors

effective contrast factor, barn ($=10^{-24}$ cm^2)	$M_w \sim 5 \times 10^4$				$M_w \sim 2.5 \times 10^5$		$M_w > 10^6$
	PSD_3H_5-1	PSD_3H_5-2	PSD_5H_3-1	PSD_5H_3-2	PSD_3H_5-3	PSD_5H_3-3	PSD_2H_6-1
$\bar{K}^2$	12.98	14.91	28.25	26.62	13.74	28.80	7.54
$\bar{K}_B^2$		7.99		0.088	7.99	0.088	4.31
$\bar{K}_\phi^2$		1.07		29.77	0.77	32.07	0.45
$2\bar{K}_B\bar{K}_\phi$		5.85		-3.24	4.98	-3.36	2.78
τ (% D)	$\tau_\phi \sim 2$	$\tau_\phi \sim 7$	$\tau_\phi \sim 95$	$\tau_\phi \sim 92$	$\tau_\phi \sim 4$	$\tau_\phi \sim 96$	$\tau_B \sim 76$

The values of the contrast factors are listed in Table III; defects in deuteriation have been neglected. The exact weights of S_B, S_ϕ, and $S_{B\phi}$ on the structure factor of the chain are given by the ratios K_B^2/K^2, K_ϕ^2/K^2, and $2K_BK_\phi/K^2$, respectively. Their relative importance depends on the type of labeling. In particular, when PSD_3H_5 and PSD_2H_6 are used, the main contribution comes from the backbone. However, the cross term also plays a role, and the effect of phenyl rings on the structure factor of the chain cannot be neglected.

2. Effect of Deuteriation Defects on Contrast Factors. The uncertainties in the degrees of deuteriation of polystyrenes influence the contrast factors. This is demonstrated in Figure 3. Indeed, from the contrast factors listed in Table III, the effect of phenyl rings on the structure factor of polystyrene is expected to be greater for PSD_2H_6 than for PSD_3H_5. This is not observed and the scattering behavior of PSD_3H_5 and PSD_2H_6 are nearly identical. This can only be explained by taking into account the effective deuteriation of these samples.

a. At small q values, an isotopic exchange ratio slightly different from unity will not distort the scattering curve. On the other hand, the contrast factor K^2, involved in the normalization of data, may be modified. Then the coherent differential cross section of one single chain will be written as

$$\Sigma^{coh}(q) = \bar{K}^2 S(q) \tag{12}$$

where $S(q)$ is the structure factor of the chain which does not depend on the labeling and $\bar{K}^2$ is the effective contrast factor which depends on the degrees of deuteriation τ_B and τ_ϕ of the backbone and phenyl rings.

For fully deuteriated polystyrenes, labeling defects are negligible, and the effective contrast factors $\bar{K}^2$ correspond to the value of K^2 given in Table III. Indeed, distinct PSD_8 samples lead to the same structure factor $g(q)$ defined by eq 2 when data are normalized to the contrast. For polystyrenes deuteriated either in the backbone or in phenyl rings, the values of $\bar{K}^2$ can then be obtained by assuming their structure factors $g(q)$ to be identical with that of fully deuteriated polystyrenes. In practice, the characteristic plateaus that appear in the modified Kratky plot of Figure 3 should be identical for the three kinds of labeled macromolecules. The molar mass of monomers is assumed to be unaffected by labeling defects. The effective contrast factors, obtained following this method, are listed in Table IV. To check that these values are consistent with the degrees of deuteriation obtained from H and D

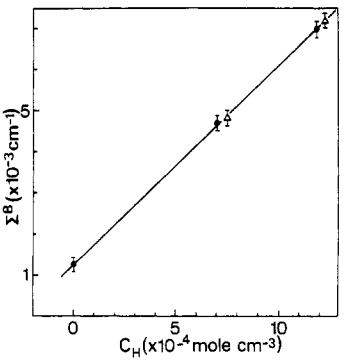

Figure 5. Background terms Σ^B obtained from dilute solutions of PSH_8 in CS_2 vs. the concentration of hydrogen atoms C_H.

NMR (Table I), we have to express $\bar{K}^2$ with respect to τ_B and τ_ϕ. So, we have considered each polystyrene as a copolymer having n_d monomers carrying the same labeling defect for a total number of monomers n. The mean scattering length density is then

$$\bar{\rho} = \frac{n - n_d}{n}\rho + \frac{n_d}{n}\rho_d \tag{13}$$

where ρ and ρ_d are the scattering length densities of the monomers without and with labeling defect, respectively, and the effective contrast factor $\bar{K}^2$ is

$$\bar{K}^2 = [K + (n_d/n)(K_d - K)]^2 \tag{14}$$

where K^2 and K_d^2 are the contrast factors of the monomers without and with labeling defect. To obtain the relation between n_d/n and τ_B or τ_ϕ for each kind of selectively deuteriated polystyrene, other arguments are needed.

For polystyrenes deuteriated in the backbone prepared from perdeuteriated polystyrenes by catalytic deuterium exchange of the phenyl groups, steric restrictions suggest that monomers with the labeling defect have the chemical formula of I. Therefore, we have

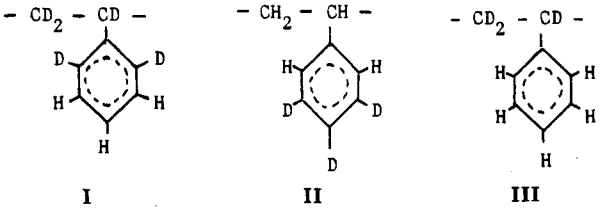

I II III

$$\frac{n_d}{n} = \frac{5}{2}\tau_\phi \quad (15)$$

with $K^2 = 12.24$ barn and $K_d^2 = 31.08$ barn.

For polystyrenes deuteriated in the phenyl rings obtained from hydrogenated polystyrenes by the same procedure, monomers with the labeling defect can be assumed to be that shown as II, and we have

$$\frac{n_d}{n} = \frac{5}{2}(1 - \tau_\phi) \quad (16)$$

with $K^2 = 31.08$ barn and $K_d^2 = 12.24$ barn.

Finally, for polystyrenes deuteriated in the backbone obtained from anionic polymerization of selectively deuteriated styrene molecules, we assume that phenyl rings have no deuterium atom and the monomer with the labeling defect is that shown as III. This leads to

$$\frac{n_d}{n} = 3\tau_B - 2 \quad (17)$$

with $K^2 = 6.02$ barn and $K_d^2 = 12.24$ barn.

b. At high q values, the scattering curves are distorted by deuteriation defects. This can be taken into account by using the relation

$$\Sigma^{coh}(q) = \bar{K}_B^2 S_B(q) + \bar{K}_\phi^2 S_\phi(q) + 2\bar{K}_B\bar{K}_\phi S_{B\phi}(q) \quad (18)$$

where the correlation functions S_B, S_ϕ, and $S_{B\phi}$ do not depend on the type of labeling but their weights, $\bar{K}_B^2$, $\bar{K}_\phi^2$, and $2\bar{K}_B\bar{K}_\phi$, in the structure factor of the chain can be modified by deuteriation defects. The effective contrast factor $\bar{K}^2$ obtained in the low q range is connected to these weights by the relation

$$\bar{K}^2 = \bar{K}_B^2 + \bar{K}_\phi^2 + 2\bar{K}_B\bar{K}_\phi \quad (19)$$

To obtain $\bar{K}_B$ and $\bar{K}_\phi$, additional assumptions, related to the previous arguments, are then needed. For low molecular weights samples, i.e., PSD_5H_3 and PSD_3H_5 with M_w close to 5×10^4 and 2.5×10^5, due to the method used for the isotopic exchange, we assume that the labeling of the backbone part of the chain is without defect. Therefore $\bar{K}_B^2$ is identical with K_B^2 given in Table III, and $\bar{K}_\phi$ is obtained by solving eq 19.

For the high molecular weight PSD_2H_6 sample, we assume that the phenyl ring part is without defect. Therefore $\bar{K}_\phi^2$ is identical with K_ϕ^2 given in Table III, and $\bar{K}_B$ is obtained by solving eq 19.

All the effective contrast factors, as well as the degrees of deuteriation estimated according to the assumptions described in **a**, are listed in Table IV. Their determination required well-normalized data, and special care was exercised to make accurate transmission measurements. Finally, these values are consistent with the results of the contrast variation method described in section IV.

3. Background Subtractions. To obtain $\Sigma^{coh}(q)$, the flat background Σ^B has to be removed from $\Sigma(q)$. For this purpose, depending on the signal-to-noise ratio of the experiment, a precise measurement of the Σ^B terms is required in order to extend the data to high scattering vectors. Specifically, we have to show that the differences observed between the correlation functions $g(q)$ of the three kinds of deuteriated polystyrenes cannot be due to a bad background subtraction.

Without the use of the polarized neutron scattering technique, Σ^B can be subtracted by taking a proper background spectrum. Obviously an ideal background spectrum is that of a sample containing the same molecules as the sample under study but without the structure. Another way is to cancel the contrast, and this goal can be reached by using a dilute solution of hydrogenated polystyrenes in carbon disulfide. Indeed, the contrast between the monomer–C_8H_8– and the CS_2 molecule is very low (see Table III), and the coherent part of the scattering is quite negligible. The exact weights of the samples are known, and it is enough to put in each case the same hydrogen atoms and the equivalent of deuterium atoms (taking the incoherent cross sections ratio $\sigma^{inc}(H)/\sigma^{inc}(D) = 38$) by using PSH_8 in CS_2. One advantage of this procedure is the capability to use, for the background spectrum, a system which is very similar to the sample studied from a dynamical point of view. We can then neglect the difference that could be due to inelastic effects.

Due to a nonexact matching of the average scattering length density of –C_8H_8– by CS_2, there is in fact a small amount of coherent scattering. However, this is not disturbing because it takes place in the range of small q values, where the signal-to-noise ratio is large enough. On the other hand, we can measure Σ^B at higher q values where the background spectrum is flat. In this way we have measured Σ^B on an absolute scale with respect to the concentration C_H of hydrogen atoms belonging to PSH_8 in dilute solution of CS_2. This dependence was expected to be linear and is presented in Figure 5. The results show that multiple scattering was then negligible. The slope of this line provides a value of $\sigma^{inc}(H)$ for the H atoms belonging to PSH_8 at the wavelength of the experiments

$$\Sigma^B = \frac{\sigma^{inc}(H)}{4\pi} N C_H + \Sigma_0^B \quad (20)$$

where Σ_0^B (cm^{-1}) is the differential cross section of the carbon disulfide, N Avogadro's number, C_H the concentration of hydrogen atoms (mol cm^{-3}), and $\sigma^{inc}(H)$ the effective incoherent cross section of the hydrogen nuclei in our experimental conditions. We obtain $\sigma^{inc}(H) = 103 \pm 7$ barn for $\lambda = 10$ Å. This value is different from the one referred to a rigidly bound hydrogen atom $\sigma^{inc}(H) = 79.7$ barn[29] and can be explained by inelastic effects as in the case of H_2O for which $\sigma^{inc}(H) = 125$ barn at room temperature and for $\lambda = 10$ Å. From this point of view we note that the method which computes the Σ^B term from the tabulated value of $\sigma^{inc}(H)$ is not correct. In our case it would lead to a larger difference between the scattering behaviors of the polystyrenes fully deuteriated and deuteriated in the backbone than those reported in section II.

What are the uncertainties in the background data $\Delta\Sigma^B$ with respect to the differences $\Sigma(q) - \Sigma^B$? For each kind of deuteriated sample, three contributions to $\Delta\Sigma^B$ have to be considered: mainly, the uncertainty related to the statistics of the background data, which is reported in Figure 5; the uncertainty related to the transmission measurements; and, finally, the uncertainty related to the degree of deuteriation and the concentration of the sample. Taking into account these three terms, we obtain characteristic ratios $\Delta\Sigma^B/(\Sigma - \Sigma^B)$, which are less than 2% at $q = 0.3$ Å^{-1} for the PSD_8 samples. For polystyrenes deuteriated either in the backbone or in the phenyl rings, they are of this order for $q = 0.15$ Å^{-1} but increase to 4% at $q = 0.3$ Å^{-1}. The scattering behaviors are then not disturbed by the uncertainties in the background spectra at least for $q < 0.3$ Å^{-1} with PSD_8 and $q < 0.15$ Å^{-1} with PSD_5H_3, PSD_3H_5, and PSD_2H_6. Their accuracy is mainly governed by the statistics of the data which lead to $\Delta g(q)/g(q) < 2\%$. From $q = 0.15$ Å^{-1}, $\Delta\Sigma^B$ begins to play a role for partially deuteriated polystyrenes, but the uncertainty in the structure factors $g(q)$ is less than 5% until $q = 0.3$ Å^{-1}. This remains reasonable and cannot explain the difference observed between the scattering behaviors of the various

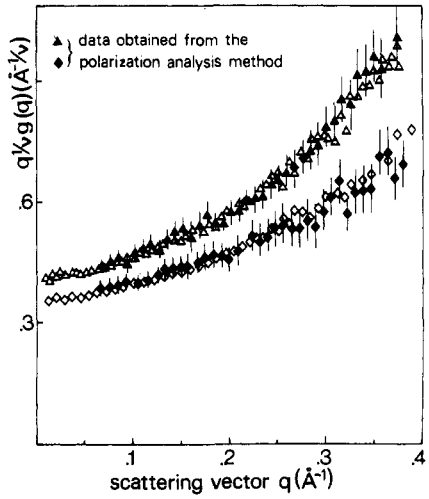

Figure 6. Scattering functions for polystyrenes deuteriated in the backbone previously shown in Figure 3 are compared to those obtained from the polarization analysis method: (Δ) PSD_2H_6-1; (◇) PSD_3H_5-3.

labeled polystyrenes. As an example, to obtain for PSD_3H_5 the same scattering behavior as for PSD_8, we should subtract a virtual background that corresponds to an uncertainty $\Delta\Sigma^B/\Sigma^B$ of 40%, leading to $\Delta\Sigma^B/(\Sigma - \Sigma^B) = 0.15\%$ at $q = 0.15$ Å^{-1}. This is quite unlikely since the related uncertainty in concentration should be $\Delta C_H/C_H = 50\%$. Increasing the spatial resolution decreases the accuracy in the structure factors. However, with the spectrometer D 1B, data obtained in the q range $0.8 < q < 1.5$ Å^{-1} were used to refine background subtractions. Indeed, at high q values, the coherent differential cross section $\Sigma^{coh}(q)$ must go to zero, and we can adjust the background term Σ^B to $\Sigma(q)$ for each sample.

Finally, the polarization analysis method has been used to check the scattering functions of some samples reported here.[31] This technique provides a direct way to separate the coherent and spin-incoherent scattering. The results obtained for polystyrenes deuteriated in the backbone, from the spectrometer IN 11 at ILL, are presented in Figure 6. The agreement with the structure factors given in Figure 3 is quite good.

4. Effects of Intermolecular Correlations and Polydispersity of Samples on Scattering Curves. The scattering functions $g(q,c)$ shown in Figure 2 do not correspond to the structure factors of one single chain $g(q)$. Intermolecular correlations are present and have to be removed before the scattering data can be interpreted. This correction, which is important at small q values only, allows us to observe for $q < 0.05$ Å^{-1} the $q^{-1/\nu}$ scattering behavior of polystyrenes deuteriated in the backbone.

To measure $g(q)$ and the intermolecular term $g_2(q,c)$ by neutron scattering, one approach is to use various mixtures of identical deuteriated and hydrogenated molecules at fixed total concentration c. This has the advantage of avoiding theoretical models and can therefore be applied at any c value. The simplest experiment is to use a solvent that has the same scattering length density as one of these molecules.[32] Then eq 4 is replaced by

$$(1/x)g(q,c) = g(q) + xg_2(q,c) \qquad (21)$$

where x is the fraction of the molecules that give interferences, and to obtain $g(q)$ and $g_2(q,c)$, only two distinct x values have to be considered.

In practice, several scattering curves corresponding to different x values are measured and a graphical method is used. However, the linearity of eq 21 has to be fulfilled

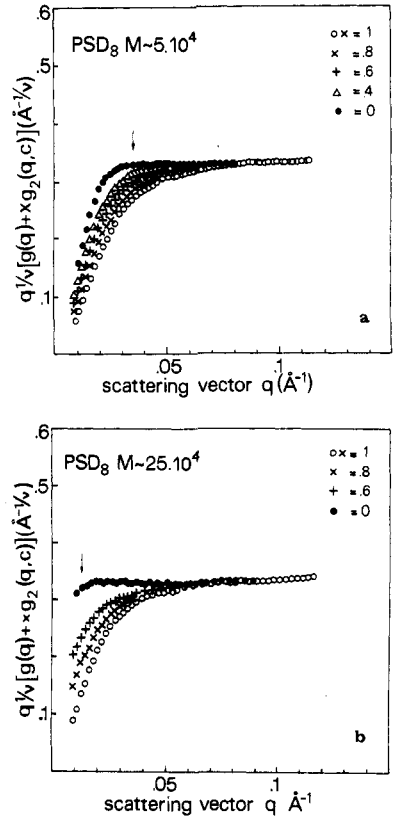

Figure 7. Effect of intermolecular correlations on the scattering curves of PSD_8 in CS_2 for $c = 0.025$ g cm^{-3}. Data are plotted in the same way as in Figure 3. $x = 0$ represents the extrapolated case, and arrows point out the q values corresponding to $qR_G = 3$: (a) molecular weight close to 5×10^4, PSD_8-1; (b) molecular weight close to 2.5×10^5, PSD_8-2.

for all q values, and any difference should be related to the experimental uncertainties (in concentrations and/or transmission factors). The accuracy of the graphical method is then increased if an additional constraint is set:

$$\lim_{q\to\infty} [(1/x)g(q,c)] = g(q) \qquad (22)$$

This assumes that $g_2(q,c)$ is zero beyond a certain q value which depends on the interaction strength between molecules and the concentration c.

We have applied this method using mixtures of perdeuteriated polystyrenes in dilute solutions at $c = 2\%$ by weight for the two molecular weights 5×10^4 and 2.5×10^5. The solvent was carbon dilsulfide, and an exact matching of the hydrogenated part of these systems was not correctly achieved (see Figure 4 or Table III). The measured scattering function can then be divided into three terms, $S_{DD}(q)$, $S_{HH}(q)$, and $S_{HD}(q)$. However, the contrast between the monomer $-C_8H_8-$ and the solvent molecule is much smaller than that of the monomer $-C_8D_8-$ (see Table III; note that this is not true for the monomer $-C_8D_3H_5-$). $S_{HH}(q)$ was therefore negligible and $S_{HD}(q)$ represented only 2.5% of the coherent scattering function for $x = 0.4$, which was the most unfavorable case in our experiments.

The effect of $g_2(q,c)$ on the scattering functions $g(q,c)$ is shown in Figure 7. Obviously $g_2(q,c)$ can be neglected for $q > 0.075$ Å^{-1} with M_w close to 5×10^4 and for $q > 0.065$ Å^{-1} with M_w close to 2.5×10^5. Thus condition 22 is met, as would be suggested by the Zimm model[33] for which

$$g_2(q,c) = -2A_2cmg^2(q) \qquad (23)$$

where c is the concentration of the polymer solution (g cm^{-3}), m the molar mass of monomers (g mol^{-1}), and A_2 the second virial coefficient (cm^3 mol g^{-2}).

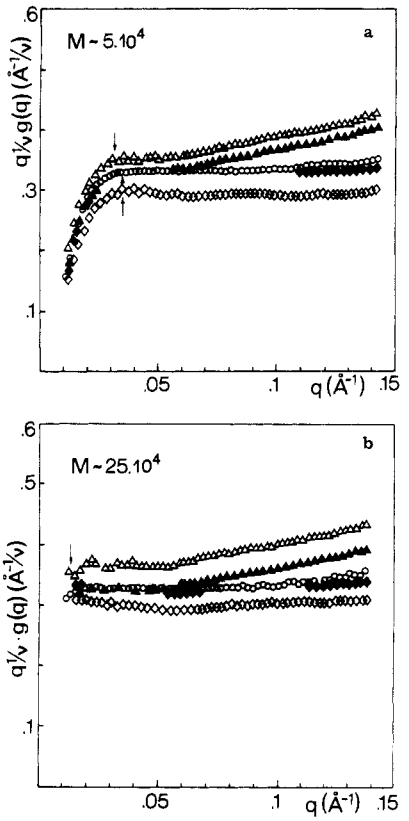

Figure 8. Intramolecular terms $g(q)$ for selectively deuteriated polystyrenes in dilute solution of CS_2: (○) fully deuteriated; (◇) deuteriated in the phenyl rings; (△) deuteriated in the backbone. Data are plotted in the same way as in Figure 3. Arrows indicate the q values corresponding to $qR_G = 3$. (a) Molecular weights close to 5×10^4: PSD_8-1, PSD_5H_3-1, and PSD_3H_5-1. Full triangles and squares are the results obtained by assuming $\tau_\phi = 0.02$ and 0.95 for PSD_3H_5 and PSD_5H_3, respectively. (b) Molecular weights close to 2.5×10^5: PSD_8-2, PSD_5H_3-3, and PSD_3H_5-3. Full triangles and squares are the results obtained by assuming $\tau_\phi = 0.04$ and 0.96 for PSD_3H_5 and PSD_5H_3, respectively.

For each class of molecular weights, we can assume that the intermolecular term $g_2(q,c)$ is the same for all our polystyrene samples, regardless of their type of labeling (such differences would only show up at high q values, when $g_2(q,c)$ becomes negligible because c is small) and of their mass (within the Zimm model the corrections are small). Then we have used the intermolecular terms $g_2(q,c)$ measured for the two molecular weights from PSD_8 to obtain the intramolecular terms $g(q)$ of PSD_3H_5 and PSD_5H_3 according to eq 21. The results are presented in Figure 8, and the characteristic $q^{-1/\nu}$ scattering behavior is found for $q < 0.05$ Å^{-1} with polystyrenes deuteriated in the backbone.

The $q^{-1/\nu}$ plateaus that appear in Figure 8 have two main features: their extension in scattering vector and their absolute height. The extension in q is related to the apparent local dimension of the chain and has already been discussed in section II. Here we discuss their heights, which for properly normed scattering curves should be identical. As explained in section III.B.2, the contrast factors depend on the degrees of deuteriation of samples, and we can estimate the values that allow the superposition of these plateaus. τ_ϕ being the degree of deuteriation of the phenyl rings, we have to assume $\tau_\phi = 0.02$ and 0.95 for PSD_3H_5 and PSD_5H_3, respectively, when molecular weights are close to 5×10^4. For molecular weights close to 2.5×10^5, we find $\tau_\phi = 0.04$ and 0.96 for the same kinds of deuteriated polystyrenes. On the other hand, the uncertainties on the degrees of deuteriation imply that the

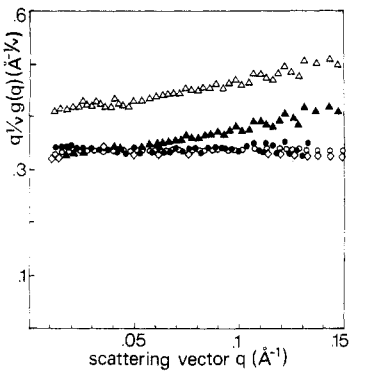

Figure 9. Scattering functions for selectively deuteriated polystyrenes with $M_w \geq 10^6$ in dilute solution of CS_2 for $c = 0.004$ g cm^{-3}: (○) PSD_8-3; (◇) PSD_5H_3-4; (△) PSD_2H_6-1. Data are plotted in the same way as in Figure 3. Intermolecular correlations are negligible in the whole experimental q range since the scattering function of PSD_8-3 in CS_2 at $c = 0.002$ g cm^{03} (filled circles) is identical with that obtained at $c = 0.004$ g cm^{-3}. Full triangles are the results obtained by assuming $\tau_B = 0.76$ for PSD_2H_6-1.

method used to remove the intermolecular term $g_2(q,c)$ for PSD_5H_3 and PSD_3H_5 is not very accurate. Indeed, a priori, it requires a good normalization of data. Therefore, for high molecular weight polystyrenes ($M_w \geq 10^6$), we performed scattering experiments at a smaller concentration, $c = 0.004$ g cm^{-3}. In this way, intermolecular correlations were found to be negligible for $q > 0.01$ Å^{-1} as checked from the perdeuteriated polystyrene by using half the concentration, 0.002 g cm^{-3}. The structure factors $g(q)$ are shown in Figure 9. The $q^{-1/\nu}$ plateau obtained from PSD_5H_3 is identical with that of PSD_8 this time, because the isotopic exchange ratio for this sample is unity. On the other hand, to superpose the $q^{-1/\nu}$ plateau obtained from PSD_2H_6, for $q < 0.05$ Å^{-1}, to that of PSD_8, we have to assume a degree of deuteriation of the backbone $\tau_B = 0.76$ (see Table IV).

Finally there could also be an effect of the sample polydispersity, which is important mostly in the Guinier range. Indeed, the q value beyond which the characteristic $q^{-1/\nu}$ (or q^{-2} if the excluded volume interaction is neglected) scattering behavior can be observed increases with the polydispersity. However, from the q value at which this $q^{-1/\nu}$ scattering behavior occurs, the effect of polydispersity can be neglected. Thus, for molecular weights close to 5×10^4 the polydispersity affects the scattering functions only below $q = 0.05$ Å^{-1}, as also expected from the values of M_w/M_n given in Table I. For molecular weights close to 2.5×10^5 it can be neglected beyond $q = 0.02$ Å^{-1}, and for molecular weights higher than 10^6 it is negligible in the whole experimental q range. This is another advantage to using samples with high molecular weight.

IV. Discussion of Results

A. Models for the Chain Structure Factor. Here we survey the models used to interpret the scattering curves of single chains to show that the results reported in section II are not surprising. Two spatial scales are considered: the intermediate range of scattering vectors defined as

$$1/R_G < q < 1/b \tag{24}$$

where R_G^2 is the mean square radius of gyration of the chain and b its statistical length;[34] and the asymptotic range of scattering vectors defined as

$$q > 1/b \tag{25}$$

1. Intermediate Range of Scattering Vectors. The first and most widely used model is that of Debye.[1] The chain is approximated by a Gaussian coil on a spatial scale

larger than the monomer size. Then, when the resolution is set to the statistical length b, the chain structure factor is

$$S(q) = (L/b)^2 P_D(qR_G) \quad (26)$$

where L is the chain contour length, assumed to be large ($L/b \gg 1$), and $P_D(q)$ is the Debye function defined as

$$P_D(qR_G) = \frac{2}{(q^2R_G^2)^2}(q^2R_G^2 + \exp(-q^2R_G^2) - 1) \quad (27)$$

In the intermediate q range, the chain may be considered as infinite and it is more convenient to use the function $g_D(q)$ defined as

$$g_D(q) = (L/b)P_D(qR_G) \quad (28)$$

since when $qR_G \gg 1$, it reduces to

$$g_D(q) = 2\left(\frac{R_G^2 b}{L}\right)^{-1}\frac{1}{q^2} \quad (29)$$

showing that $q^2g(q)$ is a constant independent of the chain contour length L (or M_w) and polydispersity because $R_G^2 b/L$ is a constant.

Several phenomenological[35-39] and formal[40-46] attempts have been made to introduce excluded volume effects in this model. With regard to $S(q)$ a scaling law has been established[13,43] and, for $qR_G \gg 1$, eq 29 is replaced by

$$g(q) = g_\infty/q^{1/\nu} \quad (30)$$

where ν is the excluded volume exponent[11-13] and g_∞ is a coefficient independent of the molecular weight and polydispersity. g_∞ depends on the detailed monomer structure and on the solvent. On the other hand, it is related to the universal constants P_∞ and $\bar{P}_\infty$ defined by

$$P(q^2R^2) = \frac{P_\infty}{\left(\frac{q^2R^2}{6}\right)^{1/2\nu}}$$
$$P(q^2R_G^2) = \frac{\bar{P}_\infty}{(q^2R_G^2)^{1/2\nu}} \quad (31)$$

where R^2 is the mean square end-to-end distance of the chain.

A simple scaling argument leads to eq 29–31. Remarkably, the characteristic $q^{-1/\nu}$ scattering behavior arises only from the L (or M_w) dependence of R^2 (or R_G^2): $R^2 \sim L^{2\nu}$. However, the universal constants P_∞ and $\bar{P}_\infty$ have different values according to the models used to describe excluded volume effects (see Appendix A). More recently they have been calculated by renormalization group methods.[44,46] For a Gaussian chain they are well-known and $P_\infty = \bar{P}_\infty = 2$.

From an experimental point of view, the difference between the scattering behavior of the two previous pictures for the chain becomes important beyond $qR_G = 3$. Below this value, the Debye function can be used to describe an experimental scattering curve even if excluded volume effects are present[45,55] when the macromolecule can be represented by a thin thread and the polydispersity is not too large. The difference between perturbed and unperturbed coils then, in a first approximation, comes only from the value of the parameter R_G^2.

These models are called universal because they do not depend on features of the monomer species. They are directly related to the random walk and the self-avoiding random walk models which are expected to be valid only for distances much longer than the statistical length b. Thus the spatial scale where the power laws 29 and 30 are realistic is not exactly the intermediate q range defined by eq 24. It corresponds rather to $1/R_G \ll q \ll 1/b$. In particular, for low molecular weights the range of scattering vectors for which eq 29 and 30 can be used vanishes, and it is no longer possible to distinguish between the two previous models by studying the scattering behavior in the intermediate q range. This is demonstrated for the atactic polystyrene in Figure 10, where the characteristic distances of the coil structure are reported.[56] It is also shown that the $q^{-1/\nu}$ scattering behavior, observed beyond $q = 0.05$ Å^{-1} with fully deuteriated polystyrenes and polystyrenes deuteriated in the phenyl rings, cannot be related a priori to the self-avoiding random walk model. Indeed, such q values correspond to $qb > 1$.

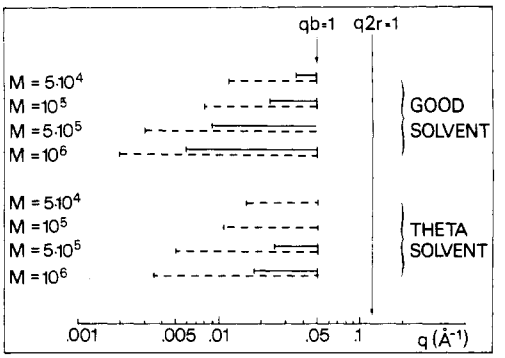

Figure 10. Characteristic distances related to the structure of atactic polystyrenes in the reciprocal space: b, statistical length; r, mean side extension of the phenyl rings from the carbon backbone; M, molecular weight. The intermediate ranges of scattering vectors defined by eq 24 are represented by dotted lines. Continuous lines represent the q ranges where the universal scattering behaviors (eq 29 and 30) are expected to be observed. In bulk or θ solvent, the power law q^{-2} is observed beyond $qR_G = 5$; in good solvent, the $q^{-1/\nu}$ scattering behavior is observed beyond $qR_G = 3$.

2. Asymptotic Range of Scattering Vectors. On a shorter spatial scale comparable with the length of a few monomers, the previous descriptions are no longer accurate and we must take into account the local properties of the chain. The structure factor obtained at larger q values will reflect these properties and is expected to differ from that of the thin flexible chain model.

These contributions can be computed in a straightforward and realistic way through the rotational isomeric state model.[16] The first calculations were made by using one atom of the backbone for each monomer as elementary scatterer. It is only recently that in the special case of polyisobutylene all pairs of atoms on the whole chain have been taken into account.[58] These calculations are correct for the chain in a vacuum but neglect the fluctuations of the solvent around the chain, which are expected to be important at high q values.[22,59]

Alternatively, analytical methods can be used. The classical approach is to divide the effect of the local structure on the scattering function of the chain into backbone and side groups parts.[22]

First, the polymer is approximated by a curve with zero thickness, and then the properties of monomer species are smoothed along this curve. On a local scale, the only parameter is the flexibility of this object.

Second, the explicit effect of side groups on the scattering function is treated as a simple thickness superimposed on the previous curve.

a. Effect of the Chain Rigidity. The effect of the chain rigidity has been extensively studied by using the Porod–Kratky wormlike chain model.[21,60] The chain is represented by a curve in space that shows a continuous transition from rod to coil by increasing its length. The

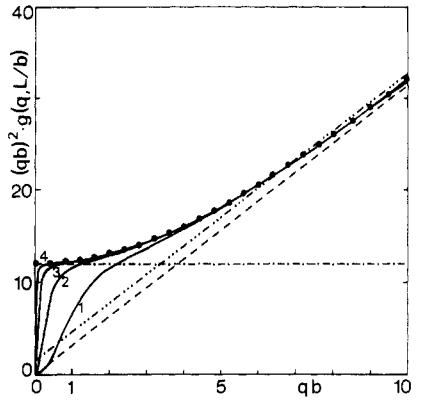

Figure 11. Kratky plot of the structure factors for the wormlike chain model, the Gaussian chain, and the rod molecule. L is the contour length, b the statistical length: (●) infinitely long wormlike chain; (—··—) asymptote for the infinitely long wormlike chain; (—·—) Debye function for $L/b = 10^4$; (- - -) rodlike molecule for $L/b = 10^4$; (—) wormlike chain for $L/b = 10$ (1), 10^2 (2), 10^3 (3), and 10^4 (4).

coil is considered Gaussian because, at the scale for which the wormlike chain model is useful, excluded volume effects are expected to be negligible. The relevant parameter is the persistence length, which characterizes the rigidity of the chain. It is half the statistical length b in the limit of the infinitely long molecule. Therefore we shall use b as a parameter and the structure factor can be written as

$$S(q) = (L/b)g(qb) \tag{32}$$

For $qb \gg 1$, $S(q)$ has the characteristic q^{-1} behavior of a rodlike molecule.[61] Des Cloizeaux has given $S(q)$ for an infinite wormlike chain in a series expansion, and its exact asymptotic law is[62]

$$\lim_{\substack{L/b\to\infty \\ q\to\infty}} g(qb) = \frac{\pi}{qb} + \frac{4}{3(qb)^2} \tag{33}$$

For finite wormlike chains, an interpolation formula has been given by Yoshizaki and Yamakawa for the structure factors $g(q,L/b)$.[63] It can be used over a large range of scattering vectors $qb < 10$ and for $0.05 < L/b < 10^4$.

These scattering functions are presented in Figure 11 and compared with those of Gaussian chain and rod molecule. It appears that to detect the characteristic plateau of the Debye model in a Kratky plot, we have to reach chain contour lengths 10^3 times larger than b. On the other hand, the q^{-1} scattering behavior is observed for $qb > 7$. The adaptation of the wormlike chain model to take into account excluded volume effects remains unsolved. We can note that this could be useful on the spatial scale corresponding to the transition from rod to coil behavior. However, the use of the Porod–Kratky model is already dubious on this scale.[31]

b. Effect of the Chain Cross Section. This effect has to be taken into account if the monomer cannot be approximated by a point scatterer. Thus, for polystyrene and from a geometrical point of view, the effect of side groups on the chain structure factor can be neglected only for $qr \ll 1$, where r is the mean side extension of side groups. At higher q values, it has to be taken into account. On a spatial scale larger than r, the polymer can be approximated by a curved cylinder of radius r, as shown in Figure 1. In our study, such a representation is reasonable because the spatial resolution of the experiments ($2\pi/q_{max}$) is coarser than 10 Å. The thickness is then described by a distribution of scattering length density around the axis of the cylinder. Let $\rho(\vec{x})$ and $\rho_S(\vec{x})$ be the distributions of scattering length density in the cross section for the polymer and the solvent, respectively; we are mainly concerned by $\Delta\rho(\vec{x}) = \rho(\vec{x}) - \rho_S(\vec{x})$, and $\rho_S(\vec{x})$ is not necessarily constant close to the polymer.[22] If we assume $\Delta\rho(\vec{x})$ to be independent of the conformation of the thin thread associated with the macromolecule and of the position along this curve, the structure factor of the chain is written as[64-66]

$$S(q) = S_0(q)\Phi(q) \tag{34}$$

where $S_0(q)$ is the scattering function for the centers of mass of the chain cross section (the optical center line) and $\Phi(q)$, the Fourier transform of the Patterson function related to $\Delta\rho(\vec{x})$. $\Phi(q)$ can be expanded as a series in the moments of these Patterson functions and we have

$$\Phi(q) = 1 - q^2R_c^2/2 + \ldots \tag{35}$$

where R_c^2 is the mean square radial radius of gyration defined as

$$R_c^2 = \frac{\int d\vec{x}\ \vec{x}^2\Delta\rho(\vec{x})}{\int d\vec{x}\ \Delta\rho(\vec{x})} \tag{36a}$$

or, in the special case of a cross section with cylindrical symmetry, as

$$R_c^2 = \frac{\int_0^\infty dx\ x^3\Delta\rho(x)}{\int_0^\infty dx\ x\Delta\rho(x)} \tag{36b}$$

Therefore R_c^2 is a real quantity that can have negative values like the apparent mean square radius of gyration of copolymers.[67] It can also be zero for some labeling situations. For $qR_c < 1$, $\Phi(q)$ can be replaced by an exponential term, and the structure factor of the chain is

$$S(q) = S_0(q)\ \exp(-q^2R_c^2/2) \tag{37}$$

which corresponds to the so-called Guinier approximation.[3] The local structure of the chain is then described by two parameters: the statistical length of the thin thread b and the mean square radius of gyration of the cross section R_c^2. To use eq 37 at higher q values, the crude assumption of a Gaussian distribution for the radial scattering elements should be required. However, the main problem in this case is that the approximation (eq 34), for the chain structure factor becomes questionable.

The introduction of the cross-section term can change drastically the structure factor of the wormlike chain, depending on the R_c^2 value. This is demonstrated in Figure 12, where the exponential approximation (eq 37) has been used for $\Phi(q)$. Its influence increases with the spatial resolution. However, for the most flexible polymer, we can expect that the effect of the cross section takes place in the q range where transition from coil to rod behavior occurs. Remarkably, for $R_c = b/5$ we obtain a scattering function that happens to agree with the Debye function in the range of scattering vectors $qb < 3$. More generally, the cross-section term can produce a large variety of scattering behaviors and, in particular, a $q^{-1/\nu}$ decay similar to that obtained from excluded volume effects. Therefore, by combining the wormlike chain model with a cross-section term, it is almost always possible to describe an experimental scattering curve in a finite q range. This can lead to erroneous results, and in section II we show how, using the neutron scattering technique, the isotopic labeling in different parts of the monomer unit can overcome these difficulties.

B. Scattering Functions of the Backbone and Phenyl Ring Parts of Polystyrene. Using the isotopic

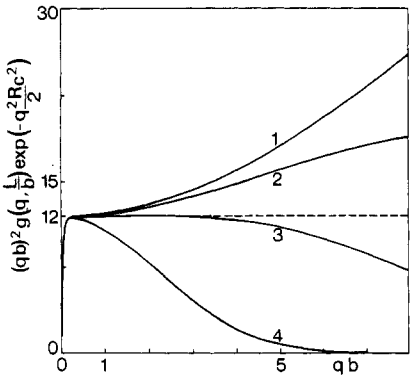

Figure 12. Effect of a cross section on the wormlike chain structure factor presented in a Kratky plot. The contour length is $L/b = 10^4$ and four R_c^2 values are considered: $R_c = 0$ (1), $b/10$ (2), $b/5$ (3), and $b/2$ (4). (Negative values for R_c^2 could be also acceptable.) Dotted curve corresponds to the Debye function.

labeling of different parts of the monomer unit, we have given different weights to the side groups in the scattering function. The next step is then to obtain the structure factor of the backbone part of the chain. This goal can be reached by using a method similar to the contrast variation technique used in biology[4] and for copolymers.[67] It is described in this section, and the model (eq 34) for the scattering function of the chain is tested.

1. Contrast Variation Method. We can consider the polystyrene as a particle with two components: the backbone (CH_2–CH) referred to as B and the phenyl rings referred to as ϕ. The coherent differential cross section per unit volume $\Sigma^{coh}(q)$ is then given by eq 9 for which three correlation functions are involved: $S_B(q)$, $S_\phi(q)$, and $S_{B\phi}(q)$. Three kinds of deuteriated polystyrene lead to three independent relations that allow the structure factor of each component to be obtained if intermolecular correlations are neglected. Taking into account the difference between the molar mass of monomers and the effect of deuteriation defects on the contrast factors, we have to solve, for each molecular weight and each q value, the following system of equations:

$$\frac{m_\alpha}{c_\alpha N}\Sigma_\alpha^{coh}(q) = \bar{K}_{B\alpha}^2 g_B(q) + \bar{K}_{\phi\alpha}^2 g_\phi(q) + 2\bar{K}_{B\alpha}\bar{K}_{\phi\alpha} g_{B\phi}(q) \quad (38)$$

α refers to PSD_8, PSD_5H_3, and PSD_3H_5 (or PSD_2H_6), c is the concentration of the polymer solution (g cm^{-3}), m is the molar mass of monomers (g mol^{-1}), and N is Avogadro's number (mol^{-1}). The values of the effective contrast factors $\bar{K}_{B\alpha}^2$, $\bar{K}_{\phi\alpha}^2$, and $2\bar{K}_{B\alpha}\bar{K}_{\phi\alpha}$ are given in Table IV. $g_B(q)$, $g_\phi(q)$, and $g_{B\phi}(q)$ are the dimensionless scattering functions normalized in the same way as those presented before (eq 2). We can note that this method, which relies on the comparison of different polymers, requires the use of the function $g(q)$ rather than the function $P(q)$. This also restricts the analysis to large enough q values when the effect of polydispersity can be neglected. Indeed, if the molar mass distributions of the macromolecules are considered, the system (eq 38) is replaced by

$$\frac{m_\alpha}{c_\alpha N}\Sigma_\alpha^{coh}(q) = \bar{K}_{B\alpha}^2\langle g_B(q)\rangle_{w_\alpha} + \bar{K}_{\phi\alpha}^2\langle g_\phi(q)\rangle_{w_\alpha} + 2\bar{K}_{B\alpha}\bar{K}_{\phi\alpha}\langle g_{B\phi}(q)\rangle_{w_\alpha} \quad (39)$$

where w_α refers to the mass distribution of the α-labeled polystyrene, and obviously to solve eq 39 we must have the same mass distribution for the different kinds of labeled macromolecules.

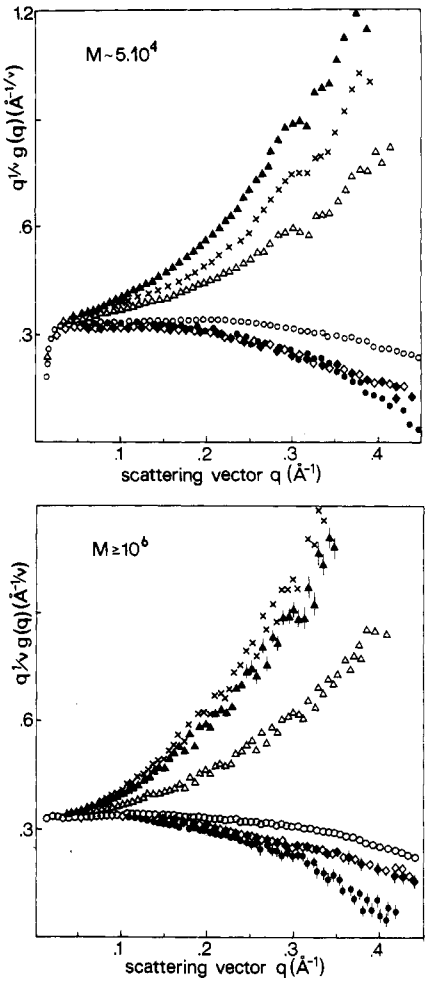

Figure 13. Correlation functions $g_B(q)$, $g_\phi(q)$, and $g_{B\phi}(q)$ obtained by solving the system of eq 38 are compared to the structure factors $g(q)$ for the three kinds of deuteriated polystyrenes: (○) fully deuteriated polystyrenes; (◇) deuteriated in the phenyl rings; (△) deuteriated in the backbone; (●) $g_{B\phi}$; (◆) g_ϕ; (▲) g_B. Crosses correspond to the correlation functions g_B obtained without taking into account deuteriation defects; in this case the results depend on the class of molecular weights. Data are plotted in the same way as in Figure 3. (a) Molecular weights close to 5×10^4: PSD_8-1, PSD_5H_3-2, and PSD_3H_5-2. (b) Molecular weights, $M_w \geq 10^6$: PSD_8-3, PSD_5H_3-4, and PSD_2H_6-1.

There is another approach in which instead of a comparison of different macromolecules a single species would be used and the scattering length density of the solvent would be varied. In this way we avoid any problem with polydispersity, and the same information can be theoretically reached because we are concerned by two components (see Appendix B). However, this method is not workable because of low contrasts and strong incoherent scattering from the solvent.

Using the coherent differential cross sections for the three kinds of deuteriated polystyrenes obtained from dilute solutions in carbon disulfide and solving for each molecular weight the system of eq 38, we have derived the correlation functions g_B, g_ϕ, and $g_{B\phi}$. The results are presented in Figure 13.

The functions $g_B(q)$ (or $g_\phi(q)$ or $g_{B\phi}(q)$) are the same for all classes of molecular weights at high q values, even though the deuteriation defects vary according to the type of deuteriated polystyrene. This shows that the corrections for deuteriation defects described in section III.B.2 are reliable.

As expected from the contrast factors, $g_\phi(q)$ is nearly identical with the structure factor $g(q)$ for PSD_5H_3, and

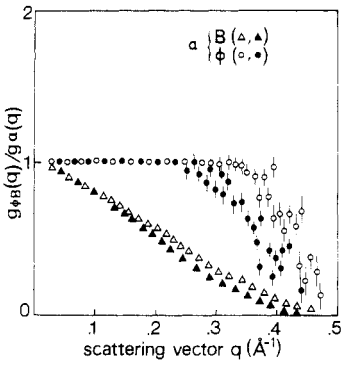

Figure 14. Plots of $g_{\phi B}(q)/g_\alpha(q)$ vs. q^2. Open triangles and circles correspond to molecular weights close to 5×10^4, and full triangles and circles correspond to molecular weights $M_w \geq 10^6$.

$g_B(q)$ is different from those corresponding to PSD_3H_5 and PSD_2H_6. In particular, in Figure 13b the $q^{-1/\nu}$ scattering behavior is no longer observed beyond $q = 0.03$ Å^{-1} for $g_B(q)$. This result shows that the monomer structure plays a role in the structure factor of polystyrene even before $q = 0.05$ Å^{-1}, as predicted by Monte Carlo computations.[16] Nevertheless, this does not allow us to conclude that the self-avoiding random walk model is no longer valid for $q > 0.03$ Å^{-1}. Indeed, the backbone part of the chain (CH_2–CH) is not necessarily the best representation of the thin thread associated to the polystyrene in our experimental conditions. In other words, to make such an assertion we should first prove that the backbone cross-section term can be neglected. At this stage we can note that measurements in θ solvent and in melts lead to the same conclusion:[31,68] the structure factor of polystyrene is affected by the structure of monomers beyond $q = 0.03$ Å^{-1}.

2. Test of the Chain Cross Section Model (Eq 34). The analysis of eq 38 describes the polymer as containing only two types of scatterers: backbone (B) and phenyl (ϕ). The simplest model for the chain cross section would assume that these scatterers are distributed with cylindrical symmetry around the central thread. Then, in the Guinier range, only two parameters would be needed to describe the cross section: a radius of gyration for the average distribution of B scatterers from the central thread and another one corresponding to ϕ scatterers. This can be tested within the frame of the pearl-necklace model[69] or alternatively by considering the scattering functions for the cross section of a cylinder. Let these functions be Φ_B for the backbone-labeled cylinder, Φ_ϕ for the phenyl-labeled cylinder, and $\Phi_{B\phi}$ for the cross term; they are products of scattered amplitudes referred to as F_B and F_ϕ for the two elementary scatterers B and ϕ, respectively, and for cylindrical symmetry we have

$$\Phi_{B\phi} = F_B F_\phi \tag{40}$$

Consequently, the scattering functions for the full cylinders are

$$\begin{aligned} g_B(q) &= g_0(q)\Phi_B(q) \\ g_\phi(q) &= g_0(q)\Phi_\phi(q) \\ g_{B\phi}(q) &= g_0(q)\Phi_{B\phi}(q) \end{aligned} \tag{41}$$

and from eq 40 they must satisfy the relationship

$$\frac{g_{\phi B}(q)}{g_B(q)} = \left(\frac{g_{\phi B}(q)}{g_\phi(q)}\right)^{-1} \tag{42}$$

Using the correlation functions g_B, g_ϕ, and $g_{B\phi}$ obtained from the data, we find that relationship 42 is not fulfilled

Table V
Mean Square Radial Radii of Gyration for Polystyrenes in Dilute Solution of Carbon Disulfide

M_w	α	$R_c^2(\alpha) - R_c^2(PSD_3H_5)$,[b] Å^2	$R_c^2(\alpha) - R_c^2(B)$,[c] Å^2	$R_c^2(\alpha)$,[d] Å^2
$\sim 5 \times 10^4$	PSD_8-1	11.6 ± 0.6	20 ± 0.8	9.6
	PSD_5H_3-2	17.4 ± 0.8	25.4 ± 1	15.3
	PSD_3H_5-2		8.6 ± 0.6	−2.3
	B[a]			−8.5
$\sim 2.5 \times 10^5$	PSD_8-2	10.4 ± 0.6	17.5 ± 0.8	9.2
	PSD_5H_3-3	17.1 ± 0.7	23.9 ± 1	15.6
	PSD_3H_5-3		6.4 ± 0.5	−1.4
	B			−7.5
M_w	α	$R_c^2(\alpha) - R_c^2(PSD_2H_6)$,[b] Å^2	$R_c^2(\alpha) - R_c^2(B)$,[c] Å^2	$R_c^2(\alpha)$,[d] Å^2
$\geq 10^6$	PSD_8-3	14.8 ± 0.8	21.6 ± 1.2	9.6
	PSD_5H_3-4	19.4 ± 1	25.9 ± 1.2	13.9
	PSD_2H_5-1		6.5 ± 0.6	−4.5
	B			−10.8

[a] B refers the backbone part of the chains. [b] From Figure 15: we obtain straight lines with two independent slopes corresponding to $-[R_c^2(\alpha) - R_c^2(\beta)]$. [c] From Figures 16: we obtain straight lines with slopes corresponding to $-[R_c^2(\alpha) - R_c^2(B)]$. [d] From fits to the wormlike chain model using the exponential approximation (eq 37).

even at small q values, as shown in Figure 14. This implies that, even in the Guinier range, more than two parameters are needed to describe the distribution of the backbone and phenyl ring groups within the cross section of the cylinder. Consequently, the three axial radii of gyration determined according to eq 37 for the three types of labeling must be independent, and the pearl-necklace model is not a good approximation for the polystyrene. A direct interpretation of this failure would be that the cross section of the chain departs markedly from cylindrical symmetry; then relation 40 does not apply. However, from a stereochemical point of view, it may make more sense to consider that the products of the scattered amplitudes F_B^2, F_ϕ^2, and $F_B F_\phi$ depend on the distance along the chemical sequence. Obviously this is not surprising but proves more especially that anisotropic correlations between the orientations of neighboring phenyl groups are not negligible.

Following the chain cross section model (eq 34), the ratio of scattering functions is related to the ratio of cross section terms

$$g_\alpha(q)/g_\beta(q) = \Phi_\alpha(q)/\Phi_\beta(q) \tag{43}$$

and in the Guinier range, i.e., at small q values, these lead to

$$\frac{g_\alpha(q)}{g_\beta(q)} = \exp\left(-\frac{q^2}{2}(R_c^2(\alpha) - R_c^2(\beta))\right) \tag{44}$$

Φ and R_c^2 being the structure factor and the mean square radius of gyration of the chain cross section.

The plot of log $(g_\alpha(q)/g_\beta(q))$ vs. q^2 is shown in Figure 15 for the different couples of deuteriated polystyrenes. We obtain straight lines providing measurements of $R_c^2(\alpha) - R_c^2(\beta)$ as given in Table V. A main point is that these straight lines are obtained in a q range larger than the one corresponding to the Guinier approximation ($qR_c < 1$), proving that the exponential approximation (eq 37) for the cross-section term can be used up to $q \sim 0.45$ Å^{-1} (or more precisely $qR_c \lesssim 1.8$) in our experimental conditions. Remarkably, among the slopes of the straight lines presented in Figure 15, only two slopes are independent: the first (triangles) is just the difference between the second (circles) and the third (squares). This proves that there is indeed a unique function $g_0(q)$ which divides the three

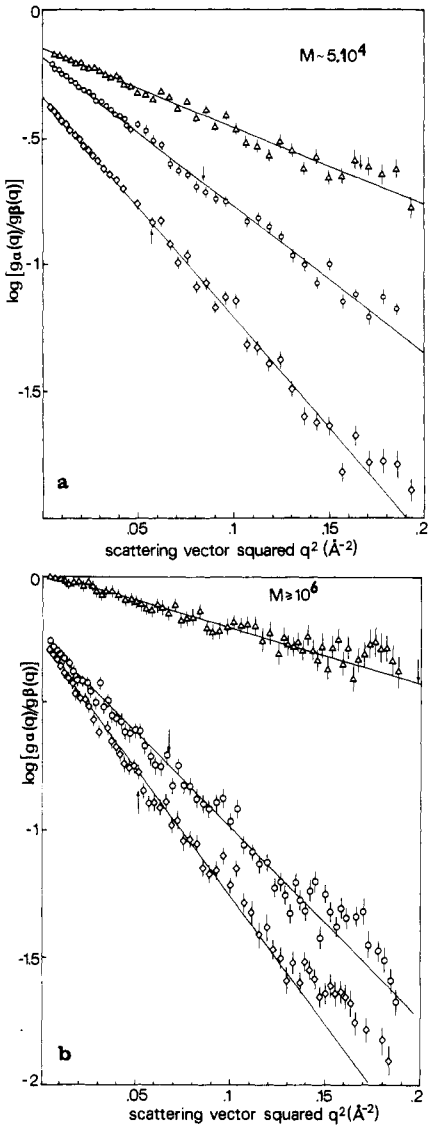

Figure 15. Plots of log $[g_\alpha(q)/g_\beta(q)]$ vs. q^2: (○) α = PSD_8 and β = PSD_3H_5 (or PSD_2H_6); (◇) α = PSD_5H_3 and β = PSD_3H_5 (or PSD_2H_6); (△) α = PSD_5H_3 and β = PSD_8. Arrows indicate the q values corresponding to $qR_c = 1$. (a) Molecular weights close to 5×10^4. (b) Molecular weights $M_w \geq 10^6$.

experimental scattering functions and yields cross-section terms which follow the Guinier law over a wide range of q values. This supports the decomposition (eq 34) when g_0 is identified as the scattering function of the thin thread. Finally, the straight line plots do not pass through the origin, showing that constant prefactors have to be considered in relation 44. However, in the present case, this point is related to the normalization of data and specifically to the effect of deuteriation defects on the contrast factors as explained in section III.A.2.

It is also instructive to compare situations that involve the backbone. The plot of log $(g_\alpha(q)/g_B(q))$ vs. q^2, where α refers PSD_8, PSD_5H_3, PSD_3H_5, and PSD_2H_6 and B is the backbone part of the chain, is presented in Figure 16. Straight lines are obtained providing measurements of $R_c^2(\alpha) - R_c^2(B)$ this time (Table V). When α denotes polystyrenes deuteriated in the backbone, data are no longer described by a simple exponential for $qR_c > 1$. Presumably the distribution of distances in the cross section of the backbone only is not as well approximated by a Gaussian as those that involve phenyl groups.

It should be useful to compare the measurements of the mean square radial radius of gyration reported here to the

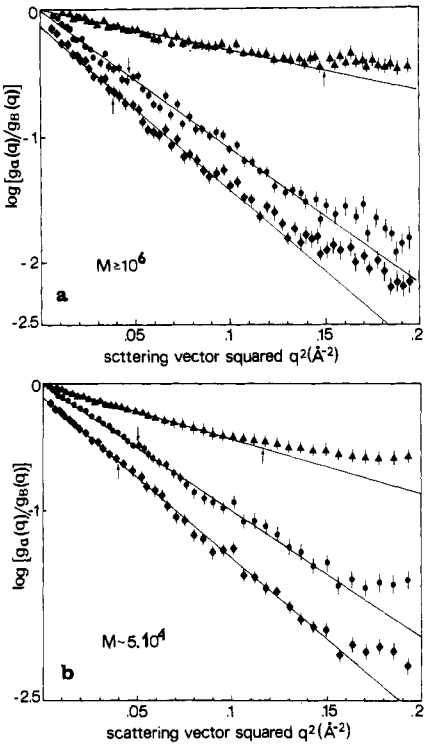

Figure 16. Plots of log $[g_\alpha(q)/g_B(q)]$ vs. q^2: (○) PSD_8; (◇) PSD_5H_3; (△) PSD_3H_5 (or PSD_2H_6). For PSD_5H_3, the straight lines are shifted in an arbitrary way along the y axis. In all cases deuteriation defects have been taken into account. Arrows indicate the q values corresponding to $qR_c = 1$. (a) molecular weights close to 5×10^4. (b) Molecular weights $M_w \geq 10^6$.

values which can be computed from a molecular model (note that the relation 36b cannot be used since the symmetry of the chain cross section is not cylindrical). For this purpose, the atactic polystyrene is not very convenient, although we can explain qualitatively the values listed in Table V. It seems better to use isotactic polystyrene for which the positions of atoms with respect to the chain axis are well-known. This is under study and should allow us, in particular, to discover whether the fluctuations of the solvent around the chain play a role.[70]

C. Fits to the Wormlike Chain Model. Once the decomposition of the chain scattering function into a thread term $g_0(q)$ and a cross-section term $\Phi(q) = \exp(-q^2R_c^2/2)$ has been checked, it is possible to use a model for $g_0(q)$ and to determine some parameters for the average conformation of the chain.

Here we use the wormlike chain model for $g_0(q)$ in a q range where excluded volume effects are expected to be negligible ($q > 0.1$ Å^{-1}). On this scale the chain contour length L played no role and three model parameters were involved: the statistical length b, the mean square radial radius of gyration R_c^2, and the mass per unit contour length M_L as experimental curves were put on an absolute scale.

By use of three different deuteriated polystyrenes, the information is expected to be increased as additional constraints are imposed: b is constant from one sample to another and M_L is related to the molar mass of monomers. The fitting procedure should then be carried out simultaneously with the three kinds of deuteriated polymers. This assumes accurately normalized data, which must be corrected for deuteriation defects. However, this has not been done in this study mainly because the statistics of the three scattering curves were not identical. The strategy was therefore to obtain the set of parameters (b, M_L, R_c^2) that reproduces in the best way the structure factor of each polystyrene and then to compare the dif-

Table VI
Universal Constants P_∞ and $\bar{P}_\infty$ for $d = 3$

			model AIII			renormalization group results to first order in $\epsilon = 4 - d$		
	model AI, $\nu = 0.588$	model AII, $\nu = 0.588$	$\nu = 0.588$, $\theta = 0.275$	$\nu = 0.588$, $\theta_1 = 0.459$	$\nu = 0.588$, $\theta_2 = 0.71$	from ref 46	from ref 44, $\nu = 0.588$	from ref 45, $\nu = 0.588$
P_∞	1.89	0.86	1.58	1.50	1.42	0.89		
$\bar{P}_\infty$	1.68	0.76	1.40	1.33	1.26		1.11	1.11

ferent results. For the three classes of molecular weights and the three types of labeling, the results have been found to be nearly identical; however, the fitting procedure was better for the scattering curves of fully deuteriated polystyrenes for which good statistics were achieved. Thus the statistical length b has been determined first from these samples and then fixed in order to measure the mean square radial radii of gyration of the other samples.

a. Fits for PSD_8. Trying to fit the data using the wormlike chain model in a finite q range, we find that several sets of parameters (b, M_L, R_c^2) can describe the scattering curves of PSD_8 within experimental accuracy. It should be reasonable to constrain one parameter, and this can be achieved through the M_L value, which is expected to be close to 44 g mol^{-1} Å^{-1}.[56] Unfortunately, the absolute measurements are not accurate enough for such a purpose. Therefore, the spatial resolution has to be improved in order to make the fitting procedure meaningful.[71] This is illustrated in Figure 17, where several b values are considered. The information content of the scattering curve at high q values is essential to obtain a reasonable accuracy, especially as the data at small q values are distorted by excluded volume effects.

Over the q range $0.15 < q < 0.6$ Å^{-1} the best fits give $b = 23 \pm 1$ Å, $M_L = 38 \pm 2$ g mol^{-1} Å^{-1}, and $R_c^2 = 9.5 \pm 0.5$ Å^2 for the three classes of molecular weights. The statistical length b is increased when the spatial resolution is lower. Indeed, over the q range $0.1 < q < 0.35$ Å^{-1} the best fits give $b = 29 \pm 1$ Å, $M_L = 42 \pm 2$ g mol^{-1} Å^{-1}, and $R_c^2 = 11.5 \pm 1$ Å^{-1}. Such behavior could be explained by the fact that excluded volume effects play a role up to $q = 0.2$ Å^{-1}. Nevertheless, the accuracy of the method seems to be too low to draw a reliable conclusion on this point. The accuracy of R_c^2 is good because its sensitivity to the fitting procedure is high. For PSD_8 R_c^2 is found to be 9.5 Å^2, and this value does not correspond to those obtained with respect to polystyrenes deuteriated in the backbone and the backbone part of the chain referred to as B. This proves that any scattering curve obtained previously does not represent the structure factor of the thin thread describing the centers of mass of the chain cross section. By fixing R_c^2 to the values obtained with respect to the backbone part of the chain and polystyrenes deuteriated in the backbone (see Table V, columns 4 and 3, respectively), it is no longer possible to fit the experimental curves of the PSD_8 samples, as shown in Figure 18.

b. Fits for Other Labeled Polystyrenes. By fixing b to 23 Å we have measured R_c^2 for the other deuteriated polystyrenes. The method was also applied to the structure factor of the backbone part of the chain, and the various fits are shown in Figure 19. The values of R_c^2 obtained in this way are listed in Table V. Their differences are in agreement with those measured by the method described in section IV.B.2, providing further support for them. Such agreements could be used as constraints to control the fitting procedure. Unfortunately, by using different b values, we always obtained the same differences between the R_c^2 values of distinct labeled polystyrenes.

Finally, R_c^2 is found to differ from zero in all cases. We conclude that no structure factor corresponds to that of the thin thread associated to the polystyrene for our experimental conditions.

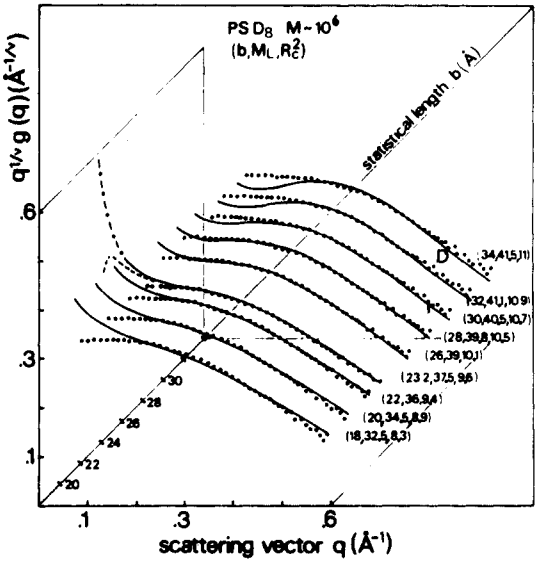

Figure 17. Fits of the scattering curve for the fully deuteriated polystyrene PSD_8-3 by the theoretical structure factor $g(q) = g_0(q) \exp(-q^2R_c^2/2)$. The wormlike chain model is assumed for $g_0(q)$. Full lines correspond to theoretical structure factors that involve b, M_L, R_c^2. The chain contour length L plays no role in the q range $0.15 < q < 0.6$Å^{-1}, as shown by considering two distinct L values (dotted lines). The best fit is obtained for $b = 23.2$ Å, $M_L = 37.5$ g mol^{-1} Å^{-1}, and $R_c^2 = 9.6$ Å^2.

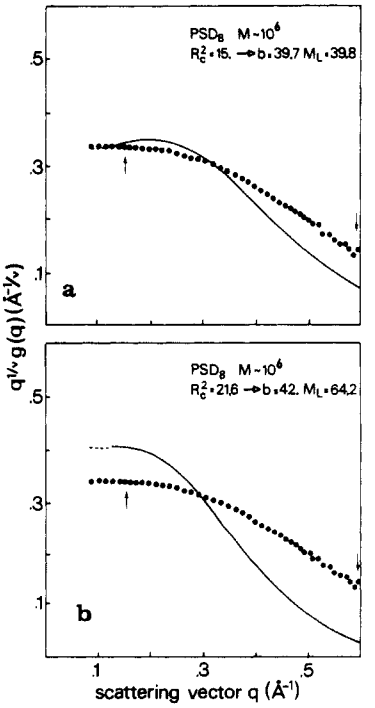

Figure 18. Fits of the scattering curve for the fully deuteriated polystyrene PSD_8-3 by the wormlike chain model. The exponential approximation (eq 37) is applied, and arrows indicate the used q range: (a) R_c^2 is fixed at 15 Å^2; (b) R_c^2 is fixed at 21.6 Å^2.

	g a	b (Å)	M_L(gmole^{-1}Å^{-1})	R_G^2(Å^2)
1	PSD_8	23	38	9.6
2	PSD_5H_3	23	37.5	15.3
3	PSD_3H_5	23	41	-2.3
4	B	23	43	-8.5

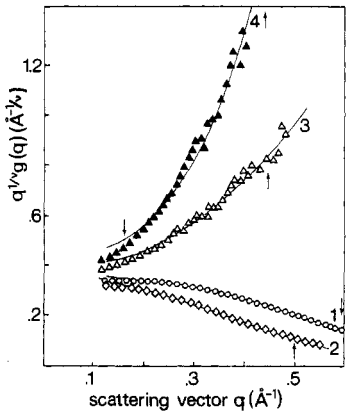

Figure 19. Fits of the scattering curves for PSD_8-1 (○), PSD_5H_3-2 (◇), PSD_3H_5-2 (△), and the backbone part of the chain B (▲) by the wormlike chain model. The exponential approximation (eq 37) is applied, and arrows indicate the used q range. b is fixed at 23 Å in all cases.

V. Conclusion

The original aim of this work was to check previous claims that the effect of local rigidity on the structure factor of the polystyrene does not show up in a q range close to the inverse of its statistical length.

By use of the neutron scattering technique, the chemical resolution was improved through the selective deuteriation of the different parts of the monomer unit. It was shown that the $q^{-1/\nu}$ scattering behavior, where ν is the excluded volume exponent, observed for q values as high as 0.1 Å^{-1} with fully deuteriated polystyrenes in dilute solution of carbon disulfide is not related to the self-avoiding random walk model. In fact, it is caused by a balance of two local effects: the rigidity of polystyrene and the side extension of its phenyl rings. Indeed, for polystyrenes selectively deuteriated in the backbone, the $q^{-1/\nu}$ scattering behavior is no longer observed beyond q = 0.05 Å^{-1}. Moreover, by use of a contrast variation method, it was shown that the monomer structure plays a role in the structure factor of the polystyrene even at smaller q values, beyond q = 0.03 Å^{-1}, in agreement with Monte Carlo simulations.[16] Therefore, the popular assumption of approximating polystyrene by an infinitely thin thread is in error for a spatial scale corresponding to distances less than 50 Å. The macromolecule is rather like a curved cylinder, and it was shown that, for $q \lesssim 0.45$ Å^{-1} in our experimental conditions, its structure factor can be approximated by the relation

$$g(q) = g_0(q)\Phi(q)$$

where $g_0(q)$ is the structure factor of the thin thread associated to the polymer and $\Phi(q)$ that of its cross section.

Concerning flexible polymers, it is not possible to measure $\Phi(q)$ from an orientation of the chains in the direction parallel to the incident beam. Thus the only tractable approach to determine $\Phi(q)$ as well as $g_0(q)$ is to use theoretical models. We have first checked that the exponential approximation eq 37 for the cross-section term is valid for $qR_c \lesssim 1.8$, allowing a comparison of scattering curves to theoretical structure factors as

$$g(q) = g_0(q)\exp(-q^2R_c^2/2)$$

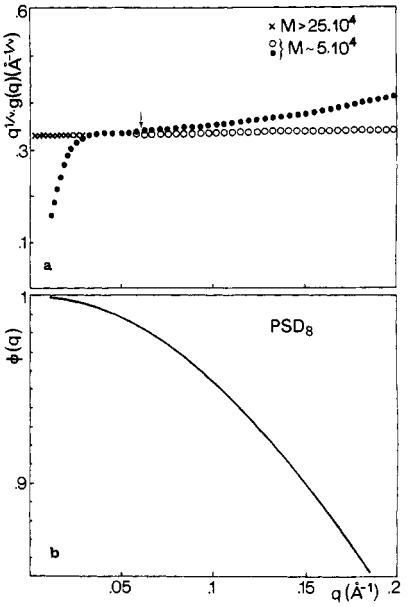

Figure 20. (a) Structure factors for the thin thread associated to polystyrene in dilute solution of CS_2 (dots and crosses). Circles correspond to the structure factor for fully deuteriated polystyrenes. Data are plotted in the same way as in Figure 3. The arrow indicates the q^* value beyond which the structure factor for the thin thread deviates from the characteristic $q^{-1/\nu}$ scattering behavior. (b) Cross-section term $\Phi(q) = \exp(-q^2R_c^2/2)$ for fully deuteriated polystyrenes: R_c^2 = 9.5 Å^2.

Then assuming the Porod–Kratky wormlike chain model for $g_0(q)$ at high q values, we have determined $\Phi(q)$ for each type of deuteriated polystyrene in dilute solution of carbon disulfide. Remarkably, these functions are not compatible with the simplest model for the chain cross section which assumes a cylindrical symmetry around the central thread; this implies more especially that anisotropic correlations between the orientations of neighboring phenyl groups are important.

The structure factor of the thin thread can then be obtained at small q values by using the above relation. Applying this method to fully deuteriated polystyrenes for which R_c^2 = 9.5 Å^2, we find that the $q^{-1/\nu}$ scattering behavior related to the self-avoiding random walk model is valid up to q^* = 0.06 Å^{-1}, as shown in Figure 20a. Beyond this q value, the transition from coil to rod behaviors is observed. It can be emphasized that this transition occurs at higher q values ($q^*b \sim 1.4$) than predicted by the wormlike chain model ($q^*b \sim 0.5$). This is not surprising because the Porod–Kratky chain model is concerned with rigid polymers and does not apply on this spatial scale.[31] On the other hand, from the cross-section term given in Figure 20b, we find that the scattering curves of fully deuteriated polystyrenes happen to follow the structure factors of the thin thread up to q = 0.1 Å^{-1} within 5% of uncertainty in our experimental conditions.

Finally, the height of the $q^{-1/\nu}$ plateau that appears in Figure 20a, $\tilde{g}_\infty$ (Å$^{-1/\nu}$), allows us to determine the universal constant $\bar{P}_\infty$ defined in section IV.A.1.

Relations 3 and 31 lead to

$$\bar{P}_\infty = m(R_G^{1/\nu}/M_w)\tilde{g}_\infty \qquad (45)$$

where m is the molar mass of monomers (g mol^{-1}), R_G the radius of gyration of the chain (Å), and M_w the chain molecular weight (g mol^{-1}). To obtain $\bar{P}_\infty$, we then have to know the prefactor A involved in the scaling law $R_G = AM_W^{\nu}$ for polystyrenes in dilute solution of carbon disulfide. From previous experimental data[15] and by using the accepted value for ν (0.588),[20,57] which has been done

all along this paper, we find $A = 0.133 \pm 0.005$ (Å $g^{-\nu}$ mol^{ν}) for perdeuteriated polystyrenes ($m = 112$ g mol^{-1}).[72] On the other hand, taking into account uncertainties of our data analysis, we have $\tilde{g}_\infty = 0.330 \pm 0.026$. Therefore, from eq 45 we obtain

$$\bar{P}_\infty = 1.20 \pm 0.17 \tag{46}$$

This result agrees with the values that can be deduced from some available published light scattering data: $\bar{P}_\infty = 1.24 \pm 0.05$ according to ref 74 and $\bar{P}_\infty = 1.29 \pm 0.04$ according to ref 55. From the relation A5, it leads to $P_\infty = 1.24 \pm 0.17$ by using eq A6 and to $P_\infty = 1.35 \pm 0.19$ by using eq A7.

These results can be compared to the values of P_∞ and $\bar{P}_\infty$ for the different models presented in Appendix A (see Table VI). They lie below the swollen Gaussian predictions, showing that the compactness of the internal structure for the thin thread is lower than that of the crude model of Peterlin.[35,36] They are rather close to the values obtained by renormalization group methods to first order in $\epsilon = 4 - d$.[44,46] However, they agree also with the values deduced from the realistic phenomenological approach given in part III of Appendix A when the exponent describing the short-range behavior of the probability distribution for two arbitrary points of the thin thread is assumed to be $\theta_2 = 0.71$.[49]

Acknowledgment. It is a pleasure for us to thank G. Beinert, B. Girard, F. Isel, and A. Lapp who prepared selectively labeled monomers and the atactic polystyrenes used in this study. Thanks are also due to B. Cabane for valuable discussions and critical reading of the manuscript. Finally, we are indebted to H. Benoit, J. P. Cotton, G. Jannink, R. C. Oberthur, and G. Weill for their suggestions.

Appendix A: Asymptotic Behavior of the Chain Structure Factor according to the Self-Avoiding Random Walk Model

Due to the scale invariance of the pair distribution of monomers, the structure factor of a long flexible polymer in a good solvent is written in the form of a scaling law. This implies a characteristic $q^{-1/\nu}$ scattering behavior for $qR_G \gg 1$, as the fractal dimension of the chain is $1/\nu$.[47] All approaches to calculate the chain structure factor according to the self-avoiding random walk model lead to this $q^{-1/\nu}$ asymptotic behavior because they assume $R_G = AM_w^{\nu}$ (or $R^2 = BL^{2\nu}$). However, they predict different prefactors and therefore different compactnesses for the internal structure of the chain. Here we survey these approaches in order to compare their resulting parameters P_∞ and $\bar{P}_\infty$ (see eq 31) for $d = 3$. We give also the renormalization group results to first order in $\epsilon = 4 - d$ for $d = 3$.

As the local properties of the chain are neglected, we set $b = 1$. On the other hand, except for the renormalization group calculations, correlations between monomers are assumed to be independent of their positions inside the chain. Therefore the probability distribution of the vector $\vec{r}$ joining two arbitrary points of the thin thread representing the polymer depends only on the contour length s between these two points. The probability distribution is denoted $p(\vec{r},s)$, and the structure factor of an infinitely long chain is written as

$$S_\infty(\vec{q}) = \int_{-\infty}^{+\infty} ds\ p(\vec{q},s) \tag{A1}$$

where $p(\vec{q},s)$ is the Fourier transform of $p(\vec{r},s)$. It may also be useful to define $S_\infty(\vec{q})$ as the Fourier transform of an effective pair distribution $\tilde{p}(\vec{r})$:

$$S_\infty(\vec{q}) = \int d\vec{r}\ e^{i\vec{q}\vec{r}}\tilde{p}(\vec{r}) \tag{A2}$$

Then we have

$$\tilde{p}(\vec{r}) = 2\int_0^{\infty} ds\ p(\vec{r},s) \tag{A3}$$

$S_\infty(\vec{q})$ allows us to obtain the asymptotic behavior of the structure factors $g(\vec{q})$ and $P(\vec{q})$ for a chain with a finite contour length L. Indeed, for $qR_G \gg 1$, we have

$$g(\vec{q}) = LP(\vec{q}) = S_\infty(\vec{q}) \tag{A4}$$

Now, from eq 31, $\bar{P}_\infty$ is related to P_∞ by the relation

$$\bar{P}_\infty = [6R_G^2/R^2]^{1/2\nu}P_\infty \tag{A5}$$

From renormalization group methods and to second order in $\epsilon = 4 - d$,[75] we have

$$\frac{6R_G^2}{R^2} = 1 - \frac{\epsilon}{96} - 0.0306\epsilon^2 \tag{A6}$$

while, by assuming a uniform swelling of all parts of the chain

$$\frac{6R_G^2}{R^2} = \frac{3}{(1+2\nu)(1+\nu)} \tag{A7}$$

I. Swollen Gaussian Chain Model. In this model[35,36] the correlations are considered to be Gaussian and the amplitude of the fluctuation $\vec{r}(s)$ only expresses the excluded volume effect. Thus

$$p(\vec{q},s) = \exp(-q^2\langle r^2(s)\rangle/6) \tag{A8}$$

and

$$\langle r^2(s)\rangle = Bs^{2\nu}$$

B is a constant that involves the local rigidity of the macromolecule and the excluded volume interaction. It is only in the Gaussian case ($\nu = {}^1/_2$) that it reduces to the statistical length b.

Using eq A8 and A1, we obtain the characteristic $q^{-1/\nu}$ scattering behavior, and the universal constants P_∞ and $\bar{P}_\infty$ depend only on the excluded volume exponent ν. We have

$$P_\infty = \frac{1}{\nu}\Gamma\left(\frac{1}{2\nu}\right) \tag{A9}$$

$\bar{P}_\infty$ is obtained by using eq A5 and A7, and the numerical values are listed in Table VI at $\nu = 0.588$, Γ being the complete gamma function.

II. Self-Consistent Field Approximation. This approach[40,41] is more formal than the previous one but does not give a realistic form for $p(\vec{r},s)$. Nevertheless, it offers a rather simple expression for $\tilde{p}(\vec{r})$. Indeed from[41] we can deduce for $d = 3$

$$\tilde{p}(\vec{r}) = \frac{2}{\nu}\frac{B^{-1/2\nu}}{4\pi}\frac{1}{r^{3-(1/\nu)}} \tag{A10}$$

with

$$\langle r^2(s)\rangle = Bs^{2\nu}$$

The characteristic $q^{-1/\nu}$ scattering behavior is then found for $qR_G \gg 1$ by using eq A10 and A2 and

$$P_\infty = \frac{2}{\nu}\left(\frac{1}{6}\right)^{1/2\nu}\Gamma\left(\frac{1}{\nu} - 1\right)\sin\left(\left[\frac{1}{\nu} - 1\right]\frac{\pi}{2}\right) \tag{A11}$$

$\bar{P}_\infty$ is obtained from eq A5 and A7, and the numerical values are listed in Table VI at $\nu = 0.588$.

III. Phenomenological Approach according to the Analogy with Critical Phenomena. This approach assumes correlations between monomers to be described by the analytical form given by Fisher for the end-to-end distance distribution $p(\vec{r},L)$.[48] It has been used by different

authors.[37,38] Here, we take into account the recent results on the probability distributions $p(\vec{r},s)$[49-51] in order to test the uniform swelling assumption.

From ref 39 and 48, we can write for $d = 3$

$$p(\vec{r},s) = C\left(\frac{1}{\langle r^2(s)\rangle}\right)^{3/2}\left(\frac{r^2}{\langle r^2(s)\rangle}\right)^{\theta/2}\exp\left[-D\left(\frac{R^2}{\langle r^2(s)\rangle}\right)^{\delta/2}\right] \quad \text{(A12)}$$

with

$$C = \frac{\delta}{4\pi}\frac{\left(\Gamma\left[\frac{\theta+5}{\delta}\right]\right)^{(\theta+3)/2}}{\left(\Gamma\left[\frac{\theta+3}{\delta}\right]\right)^{(\theta+5)/2}}$$

$$D = \left(\frac{\Gamma\left[\frac{\theta+5}{\delta}\right]}{\Gamma\left[\frac{\theta+3}{\delta}\right]}\right)^{\delta/2}$$

and

$$\langle r^2(s)\rangle = Bs^{2\nu} \quad \text{(A13)}$$

For $\theta = (\gamma - 1)/\nu$ and $\delta = 1/(1-\nu)$, eq A12 leads to short- and long-range behaviors identical with the ones determined by Des Cloizeaux for the end-to-end distance distribution[52] (actually the long-range behavior is rather

$$\left(\frac{r^2}{\langle r^2(s)\rangle}\right)^{\sigma/2}\exp\left[-D\left(\frac{r^2}{\langle r^2(s)\rangle}\right)^{\delta/2}\right]$$

but clearly the power law is negligible). On the other hand, this analytical form (eq A12), which is just the product of the short- and long-range behaviors, fits well the data obtained from exact enumeration techniques.[39,53] This is not surprising because in each region ($r < (\langle r^2(s)\rangle)^{1/2}$ or $r > (\langle r^2(s)\rangle)^{1/2}$) when one factor is rapidly varying the other is virtually constant. Finally, for $\nu = {}^1/_2$ and $\gamma = 1$ ($\theta = 0$ and $\delta = 2$) eq A12 is just the Gaussian distribution.

By using eq A2, A3, and A12, we obtain the characteristic $q^{-1/\nu}$ scattering behavior and the universal constants P_∞ and $\bar{P}_\infty$ depend on two exponents: ν and γ through θ and δ. We have

$$P_\infty = \frac{2}{\nu}\left(\frac{1}{6}\right)^{1/2\nu}\Gamma\left(\frac{1}{\nu}-1\right)\sin\left(\left[\frac{1}{\nu}-1\right]\frac{\pi}{2}\right)\times \frac{\left[\Gamma\left(\frac{\theta+5}{\delta}\right)\right]^{1/2\nu}}{\left[\Gamma\left(\frac{\theta+3}{\delta}\right)\right]^{1+(1/2\nu)}}\Gamma\left(\frac{\nu(\theta+3)-1}{\nu\delta}\right) \quad \text{(A14)}$$

$\bar{P}_\infty$ is obtained by using eq A5 and A7, and the numerical values are listed in Table VI at $\nu = 0.588$ and $\gamma = 1.1615$.

Now one could argue that the probability distribution for the distance between two arbitrary points of the chain is still written as eq A12. The long-range behavior can be considered identical with that of the end-to-end distance distribution (some differences are expected for the exponent σ[51] but they are negligible, at least for $d = 3$ as shown by numerical studies[53]). However, the exponent θ, which describes the short-range behavior, depends on the position of the two points along the chain. So by considering one point at one end and the other in the central part of the chain (situation 1) or two points in the central part (situation 2), we have respectively[49] $\theta_1 = 0.459 \pm 0.003$ and $\theta_2 = 0.71 \pm 0.05$. These results lead to different values for P_∞ and $\bar{P}_\infty$, as shown in Table VI. However, the differences are small (within 10%) and, in a first approximation, give support for the uniform swelling assumption. On the other hand, for the average conformation of a real macromolecule, the physical situation 2 is expected to be a better representation, as previously noted by Witten.[44] Indeed, most monomer pairs are in the situation 2. Moreover, an infinitely long chain is like a ring and, in this case, there is only one contact exponent that corresponds to θ_2, as demonstrated by renormalization group calculations to first order in $\epsilon = 4 - d$.[76]

Finally, we can emphasize that these differences are more important for the coefficient g_∞ defined by eq 30. Indeed, from eq 30, 31, and A4

$$g_\infty = P_\infty(6/B)^{1/2\nu} \quad \text{(A15)}$$

and B, defined by eq A13, is expected to increase from the end-to-end situation to the one referred to as 2.[51,54] Therefore, to observe differences in the correlations between monomers according to their positions inside the chain, one experimental approach would be to study the scattering behavior of different labeled parts of a chain in the intermediate q range through the coefficient g_∞.

IV. Renormalization Group Results. The renormalization group calculations avoid the uniform swelling assumption. However, they are generally restricted to the first order in $\epsilon = 4 - d$. P_∞ has been obtained by Des Cloizeaux and Duplantier.[46] For $d = 3$, its value is close to that obtained from the self-consistent field approach (see Table VI). Nevertheless, the ϵ expansions are different. $\bar{P}_\infty$ can be deduced either from the universal parameter given by Witten,[44] which is just $P_\infty/3^{1/2\nu}$, or from the structure factor $P(qR_G)$ given in a closed form to order ϵ by Oono, Ohta, and Freed.[45] The numerical values, obtained by using $\nu = 0.588$, are listed in Table VI.

Appendix B: Contrast Variation Method

The contrast variation method is useful in the study of the structure of a multicomponent particle.[4,67] It is carried out mainly by changing the scattering length density of the solvent (or the matrix) ρ_S, and with neutron scattering this is achieved through isotopic substitution. The contrast factors that control the coherent scattering can then be varied continuously. With respect to the approach using the selective deuteriation of the different parts of the particle, the advantage is that the scattering experiments can be performed on the same particle. This avoids also any fine chemical isotopic substitution of the particle subunits. However, in this way the structure factor of each part of the particle can only be obtained for a two-component particle. Indeed, the coherent differential cross section for a p-component particle in solution is

$$\Sigma^{coh}(q) = \sum_{\alpha,\beta=1}^{P} K_\alpha K_\beta S_{\alpha\beta}(q) \quad \text{(B1)}$$

with $K_\alpha = v_\alpha(\rho_\alpha - \rho_S)$, v_α being the volume of the elementary scatterer related to the α component, ρ_α its scattering length density, and $S_{\alpha\beta}(q)$ the various correlation functions to be extracted. This can be written as

$$\Sigma^{coh}(q) = \rho_S{}^2\left(\sum_{\alpha,\beta=1}^{P} v_\alpha v_\beta S_{\alpha\beta}(q)\right) - \rho_S\left(\sum_{\alpha,\beta=1}^{P} v_\alpha v_\beta(\rho_\alpha + \rho_\beta)S_{\alpha\beta}(q)\right) + \sum_{\alpha,\beta=1}^{P} v_\alpha v_\beta \rho_\alpha \rho_\beta S_{\alpha\beta}(q) \quad \text{(B2)}$$

and obviously, even if ρ_S is changed continuously, only three independent relationships between the different $S_{\alpha\beta}$ functions can be obtained if the molar volumes are known. Therefore, for more than two components the selective

labeling of the different parts of the particle has to be used, at least as a complementary way. On the other hand, for a two-component particle with scattering length densities ρ_1 and ρ_2 that are rather close (quasi-homogeneous particle), the experimental accuracy is poor because the ρ_S values of interest lead to a weak signal. The selective labeling of one part of the particle is then also required. This is the case for our study.

Registry No. Polystyrene, 9003-53-6; neutron, 12586-31-1.

References and Notes

(1) Debye, P. *J. Phys. Colloid Chem.* **1947**, *51*, 18.
(2) Flory, P. J. *Statistical Mechanics of Chain Molecules*; Wiley: New York, 1969.
(3) Guinier, A.; Fournier, G. *Small Angle Scattering of X Rays*; Wiley: New York, 1955.
(4) Jacrot, B. *Rep. Prog. Phys.* **1976**, *39*, 911.
(5) Loucheux, C.; Weill, G.; Benoit, H. *J. Chim. Phys.* **1958**, *55*, 540.
(6) Durchschlag, M.; Kratky, O.; Breitenbach, J. W.; Wolf, B. A. *Monatsh. Chem.* **1970**, *101*, 1462.
(7) Okano, K.; Wada, E.; Hiramatsu, H. *Rep. Prog. Polym. Phys. Jpn.* **1974**, *17*, 145.
(8) Garg, S. K.; Stivala, S. S. *Polymer* **1982**, *23*, 514.
(9) Cotton, J. P.; Decker, D.; Farnoux, B.; Jannink, G.; Ober, R.; Picot, C. *Phys. Rev. Lett.* **1974**, *32*, 1170.
(10) Farnoux, B. *Ann. Phys.* **1973**, *t1*, 73.
(11) Kuhn, W. *Kolloid-Z.* **1934**, *68*, 2.
(12) Flory, P. J. *Principles of Polymer Chemistry*; Cornell University; Ithaca, NY, 1953.
(13) de Gennes, P.-G. *Scaling Concepts in Polymer Physics*; Cornell University: Ithaca, NY, 1979.
(14) Wignall, G. D.; Ballard, D. G. H.; Schelten, J. *Eur. Polym. J.* **1974**, *10*, 861.
(15) Cotton, J. P.; Decker, D.; Benoit, H.; Farnoux, B.; Higgins, J. S.; Jannink, G.; Ober, R.; Picot, C.; Des Cloizeaux, J. *Macromolecules* **1974**, *7*, 863.
(16) Yoon, D. Y.; Flory, P. J. *Polymer* **1975**, *16*, 645. *Macromolecules* **1976**, *9*, 294, 299.
(17) Kirste, R. G. *Makromol. Chem.* **1967**, *101*, 91.
(18) Kirste, R. G.; Kruse, W. A.; Ibel, K. *Polymer* **1975**, *16*, 120.
(19) Farnoux, B.; Boué, F.; Cotton, J. P.; Daoud, M.; Jannink, G.; Nierlich, M.; de Gennes, P.-G. *J. Phys.* **1978**, *39*, 77.
(20) Le Guillou, J. C.; Zinn Justin, J. *Phys. Rev. Lett.* **1977**, *39*, 95.
(21) Porod, G. *Monatsh. Chem.* **1949**, *80*, 251. Kratky, O.; Porod, G. *Recl. Trav. Chim. Pays-Bas* **1949**, *68*, 1106.
(22) Kirste, R. G. *Z. Phys. Chem. (Munich)* **1963**, *36*, 265; **1964**, *42*, 351.
(23) Szwarc, M. *Makromol. Chem.* **1960**, *35*, 132. Worsfold, D. J.; Bywater, S. *Can. J. Chem.* **1960**, *38*, 1891.
(24) Wilenberg, B. *Makromol. Chem.* **1976**, *177*, 3625.
(25) Lapp, A.; Beinert, G.; Picot, C. *Makromol. Chem.* **1984**, *185*, 453.
(26) Grubisic-Gallot, Z.; Picot, M.; Gramain, Ph.; Benoit, H. *J. Appl. Polym. Sci.* **1972**, *16*, 2931.
(27) Stuhrmann, H. B. *J. Appl. Crystallogr.* **1974**, *7*, 173. Cotton, J. P.; Benoit, H. *J. Phys.* **1975**, *36*, 905.
(28) Oberthur, R. C. ILL Internal Report.
(29) Koester, L.; Rauch, H. "Summary of Neutron Scattering Lengths", IAEA Contract 2517/RB, 1981. Marshall, W.; Lovesey, S. W. *Theory of Thermal Neutron Scattering*; Oxford Clarendon: Cambridge, 1971.
(30) Van Krevelen, D. W. *Properties of Polymers*; Elsevier: New York, 1972; Chapter IV.
(31) Rawiso, M.; Boué, F.; Mezei, F., to be published.
(32) Williams, C. E.; Nierlich, M.; Cotton, J. P.; Jannink, G.; Boué, F.; Daoud, M.; Farnoux, B.; Picot, C.; de Gennes, P.-G.; Rinaudo, M.; Moan, M.; Wolff, C. *J. Polym. Sci., Polym. Lett. Ed.* **1979**, *17*, 379. Ackasu, Z.; Summerfield, G.; Jahshan, S.; Han, C.; Kim, C.; Yu, H. *J. Polym. Sci., Polym. Phys. Ed.* **1980**, *18*, 863.
(33) Zimm, B. H. *J. Chem. Phys.* **1948**, *16*, 1093.
(34) Kuhn, W. *Kolloid-Z.* **1936**, *76*, 258; **1939**, *87*, 3.
(35) Peterlin, A. *J. Chem. Phys.* **1955**, *23*, 2464.
(36) Benoit, H. *C. R. Acad. Sci.* **1957**, *245*, 2244. Ptitsyn, O. B. *Zh. Fiz. Khim.* **1957**, *31*, 1091.
(37) McIntyre, D. S.; Mazur, J.; Wims, A. M. *J. Chem. Phys.* **1968**, *49*, 2887, 2896.
(38) Utiyama, J.; Tsunashima, Y.; Kurata, M. *J. Chem. Phys.* **1971**, *55*, 3133.
(39) McKenzie, D. S. *Phys. Rep.* **1976**, *C27*, 35.
(40) Edwards, S. F. *Proc. Phys. Soc., London* **1965**, *85*, 613.
(41) de Gennes, P.-G. *Rep. Prog. Phys.* **1969**, *32*, 187.
(42) Shinbo, K.; Miyake, Y. *J. Phys. Soc. Jpn.* **1980**, *48*, 2084.
(43) Schafer, L.; Witten, T. A. *J. Chem. Phys.* **1977**, *66*, 2121. Witten, T. A.; Schafer, L. *J. Chem. Phys.* **1981**, *74*, 2582.
(44) Witten, T. A. *J. Chem. Phys.* **1982**, *76*, 3300.
(45) Oono, Y.; Ohta, T.; Freed, K. F. *Macromolecules* **1981**, *14*, 1588. Ohta, T.; Oono, Y.; Freed, K. F. *Phys. Rev. A* **1982**, *A25*, 2801.
(46) Des Cloizeaux, J.; Duplantier, B. *J. Phys. Lett.* **1982**, *46*, L457.
(47) Des Cloizeaux, J. *J. Phys.* **1981**, *42*, 635.
(48) Fisher, M. E. *J. Chem. Phys.* **1966**, *44*, 616. McKenzie, D. S.; Moore, M. A. *J. Phys. A: Gen. Phys.* **1971**, *A4*, L82.
(49) Des Cloizeaux, J. *J. Phys.* **1980**, *41*, 223.
(50) Oono, Y.; Ohta, T. *Phys. Lett.* **1981**, *A85*, 480.
(51) Duplantier, B. *J. Phys. Lett.* **1985**, *46*, L751.
(52) Des Cloizeaux, J. *Phys. Rev.* **1974**, *A10*, 1665.
(53) Redner, J. *J. Phys. A: Gen. Phys.* **1980**, *A13*, 3525.
(54) Barrett, A. J. *Macromolecules* **1984**, *17*, 1561.
(55) Kirste, R. G.; Oberthur, R. C. In *Small Angle X-ray Scattering*; Glatter, O., Kratky, O., Eds.; Academic: New York, 1982; pp 387–431.
(56) To estimate the statistical length b of atactic polystyrenes we use the relation between the mean square radius of gyration of the chain in θ solvent $R_{G\theta}^2$ and the molecular weight M_w. It can be written as $R_{G\theta}^2/M_w = b/6M_L$, and we have to know the mass per unit contour length M_L independently. Considering the zigzag carbon skeleton, we obtain a contour length per monomer of 2.52 Å. This leads to M_L = 41.2 g mol^{-1} Å^{-1} for hydrogenated polystyrenes. From light scattering experiments,[57] $R_{G\theta} = 0.290\ M_w^{0.5}$ for hydrogenated polystyrenes, we have M_L/b = 1.98 g mol^{-1} Å^{-1}, and we obtain b = 20.8 Å. From neutron scattering,[15] $R_{G\theta} = 0.294\ M_w^{0.5}$ for hydrogenated polystyrenes, we have M_L/b = 1.93 g mol^{-1} Å^{-1}, and we obtain b = 21.4 Å. Accordingly and by taking into account the temperature dependence, b = 20 Å seems to be a reasonable value for the statistical length of atactic polystyrenes at room temperature.
(57) Cotton, J. P. *J. Phys. Lett.* **1980**, *41*, L231.
(58) Hayashi, H.; Flory, P. J.; Wignall, G. D. *Macromolecules* **1983**, *16*, 1328.
(59) Kirste, R. G.; Wunderlich, W. *Makromol. Chem.* **1964**, *73*, 240.
(60) Daniels, H. E. *Proc. R. Soc. Edinburgh* **1952**, *63*, 290. Hermans, J. J.; Ullman, R. *Physica (Amsterdam)* **1952**, *18*, 951.
(61) Neugebauer, T. *Ann. Phys.* **1943**, *42*, 509.
(62) Des Cloizeaux, J. *Macromolecules* **1973**, *6*, 403.
(63) Yoshizaki, T.; Yamakawa, H. *Macromolecules* **1980**, *13*, 1518.
(64) Kratky, O. *Z. Electrochem.* **1956**, *60*, 245. Luzzati, V. *Acta Crystallogr.* **1960**, *13*, 939.
(65) Koyama, R. *J. Phys. Soc. Jpn.* **1974**, *36*, 1409.
(66) Porod, G. In *Small Angle X-Ray Scattering*; Glatter, O., Kratky, O., Eds.; Academic: New York, 1982; pp 17–51.
(67) Ionescu, L.; Picot, C.; Duval, M.; Duplessix, R.; Benoit, H.; Cotton, J. P. *J. Polym. Sci.* **1981**, *19*, 1019.
(68) Coulon, G.; Lefebvre, J. M.; Picot, C.; Rawiso, M., to be published.
(69) Debye, P. *Phys. Z.* **1930**, *31*, 419. Burchard, W.; Kajiwara, K. *Proc. R. Soc. London, A* **1970**, *A316*, 185.
(70) Rawiso, M.; Oberthur, R. C.; Schaerpf, O.; Lapp, A., to be published.
(71) Luzzati, V.; Tardieu, A. *Annu. Rev. Biophys. Bioeng.* **1980**, *9*, 1.
(72) As mentioned in section III.A.1, using a least-squares fit of data presented in ref 15, we deduce the law $\langle R_G \rangle_Z$ (Å) = 0.122 $M_w^{0.6}$ (g mol^{-1}) for perdeuteriated polystyrenes in dilute solution of carbon disulfide. However, the data can also be described by the law $\langle R_G \rangle_Z$ (Å) = (0.145 ± 0.005)$M_w^{0.588}$ (g mol^{-1}) within experimental accuracy. Moreover, correcting the data for polydispersity effects according to the method proposed by Oberthur,[73] we obtain R_G (Å) = (0.133 ± 0.005)$M_w^{0.588}$ (g mol^{-1}). We note that the prefactor depends drastically on the exponent and polydispersity.
(73) Oberthur, R. C. *Makromol. Chem.* **1978**, *179*, 2693.
(74) Noda, I.; Imai, M.; Kitano, T.; Nagasawa, M. *Macromolecules* **1983**, *16*, 425.
(75) Benhamou, M.; Mahoux, G. *J. Phys. Lett.* **1985**, *46*, L689.
(76) Lipkin, M.; Oono, Y.; Freed, K. F. *Macromolecules* **1981**, *14*, 1270.